

## Supporting Information

### The effect of enhanced $\pi$ - $\pi$ interactions and tail branching on azobenzene surfactant self-assembly

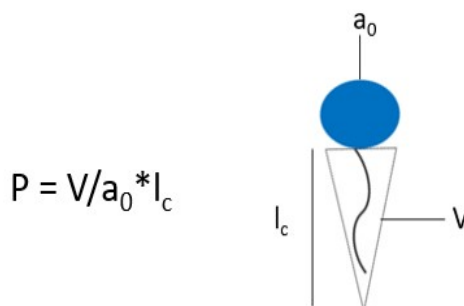
Mehmoona Zaib,<sup>a</sup> Jonathan M. Faber,<sup>a</sup> Ashley P. Williams,<sup>a</sup> Anna V. Sokolova,<sup>b</sup> Rico F. Tabor<sup>a\*</sup> and Kellie L. Tuck<sup>a\*</sup>

a. School of Chemistry, Monash University, Victoria 3800, Australia, E-mail: Kellie.Tuck@monash.edu, Rico.Tabor@monash.edu.

b. Australian Centre for Neutron Scattering, ANSTO, Lucas Heights, NSW 2234, Australia

#### Critical packing parameter $P$ calculation

The critical packing parameter ( $P$ ) was calculated following a previously established procedure.<sup>1</sup> Initially, molecular structures were drawn using Chem3D, and their 3D geometries were optimized via the built-in MM2 force field. The tail group length was then measured using Chem3D's internal measuring tool. The betaine head group was removed to isolate the tail volume, and the optimized tail structures were exported as .sdf files. These files were submitted to the Molecular Volume Calculator provided by the Supercomputing Facility for Bioinformatics and Computational Biology at IIT Delhi [<https://scfbio-iitd.res.in/Sanjeevini/Molecular-volume-calculator.php>] to obtain the tail volumes for both *cis* and *trans* isomers. The minimum interfacial area per betaine head group was obtained from reported experimental values from the literature. Using the calculated tail volume and length along with the estimated head group area, the critical packing parameter ( $P$ ) for each azo-



surfactant was determined using the standard formula.

Figure S1: Critical packing parameter ( $P$ ), where  $V$  is the volume of the hydrophobic tail,  $a_0$  is surface area of head, and  $l_c$  is the length of the hydrophobic tail.

**Table S1:** Critical packing parameter  $P$  calculation

| Surfactant       | $a_0$ (Å <sup>2</sup> ) | $V_{\text{trans}}$ (Å <sup>3</sup> ) | $V_{\text{cis}}$ (Å <sup>3</sup> ) | $l_{\text{c(trans)}}$ Å | $l_{\text{c(cis)}}$ Å | $P_{\text{trans}}$ | $P_{\text{cis}}$ |
|------------------|-------------------------|--------------------------------------|------------------------------------|-------------------------|-----------------------|--------------------|------------------|
| <i>n</i> -BDAP   | 55.5                    | 250.35                               | 250.00                             | 16.8                    | 12.2                  | 0.27               | 0.37             |
| <i>iso</i> -BDAP | 55.5                    | 250.29                               | 248.73                             | 14.7                    | 10.4                  | 0.31               | 0.43             |
| <i>t</i> -BDAP   | 55.5                    | 250.10                               | 249.62                             | 14.6                    | 12.6                  | 0.31               | 0.36             |
| <i>n</i> -BDAN   | 55.5                    | 289.43                               | 288.98                             | 16.7                    | 13.1                  | 0.31               | 0.40             |
| <i>iso</i> -BDAN | 55.5                    | 289.35                               | 288.78                             | 14.6                    | 11                    | 0.36               | 0.47             |
| <i>t</i> -BDAN   | 55.5                    | 289.07                               | 287.82                             | 13.2                    | 12.2                  | 0.39               | 0.42             |

### Photoisomerisation and kinetic studies

UV–vis spectroscopy was used to evaluate the photo-isomerisation and thermal stability behaviour of the azo-surfactants 0.1 M solutions of *n*-BDAN, *iso*-BDAN, *t*-BDAN and *n*-BDAP. The *trans*-rich photostationary state (PSS) was achieved through thermal relaxation by heating the sample solution to 50 °C, followed by storage in the dark until it cooled to room temperature. Upon irradiation at 365 nm, rapid photoisomerisation to a *cis*-rich state occurred, reaching equilibrium within 5 minutes. Complete conversion to the *cis*-isomer is limited by spectral overlap between the  $\pi \rightarrow \pi^*$  (*trans*) and  $n \rightarrow \pi^*$  (*cis*) transitions. The *cis*-isomer fraction ( $P_{\text{cis}}$ ) was calculated using the change in absorbance at 386, 387, 392 or 348 nm for *n*-BDAN, *iso*-BDAN, *t*-BDAN or *n*-BDAP respectively, using the following equation. Relaxation back to *trans*-dominant PSS was monitored by UV-Vis spectroscopy in the dark, at the wavelengths noted in Fig. S2.

$$P_{\text{cis}} = A_i - A_f \div A_i * 100$$

where  $P_{\text{cis}}$  is the proportion of the *cis* isomer present,  $A_i$  is the absorbance noted in Fig. S2 before UV irradiation, and  $A_f$  is the absorbance after UV irradiation.

The relaxation processes for all surfactants followed first-order reaction kinetics, which is consistent with a unimolecular process driven by light absorption.<sup>2, 3</sup> The rate constants, determined from the linear fit of  $\ln(A_t/A_0)$  vs time, as well as the half-lives, are noted in Table S2.

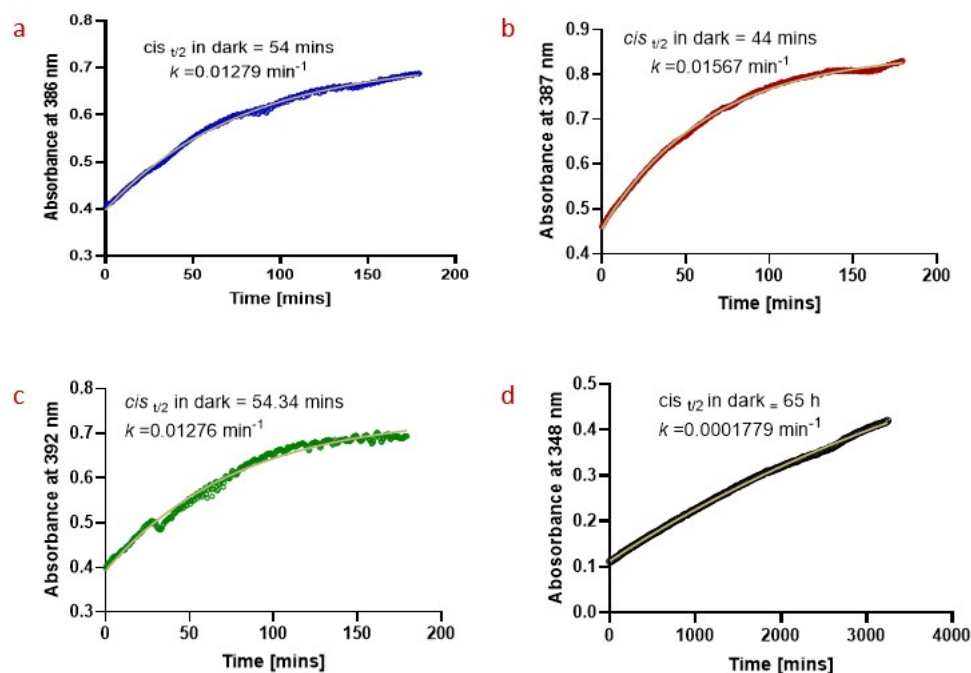


Figure S2:

Change in absorbance of samples after irradiation at 365 nm a) *n*-BDAN b) *iso*-BDAN c) *tert*-BDAN d) *n*-BDAP

**Table S2:** Thermal relaxation kinetic data

| Surfactant        | Rate constant ( <i>k</i> )<br>(min <sup>-1</sup> ) | <i>t</i> <sub>1/2</sub> (min) |
|-------------------|--|-------------------------------|
| <i>n</i> -BDAN    | 0.013  | 54.2                          |
| <i>iso</i> -BDAN  | 0.016  | 44.2                          |
| <i>tert</i> -BDAN | 0.013  | 54.3                          |
| <i>n</i> -BDAP    | 0.00018  | 3896 (65 h)                   |

The reversibility of photoresponsiveness of 0.1 M *n*-BDAN under alternating UV (365 nm) and visible light irradiation is shown in Fig. S3. Illumination with UV This reversible switching between the *trans*- and *cis*-rich PSS over five successive irradiation cycles demonstrate excellent cyclability; however, a slight decrease in absorbance of the *trans* band after repeated cycling indicates formation of a new steady-state equilibrium that is less *trans*-rich than the initial *trans* state.

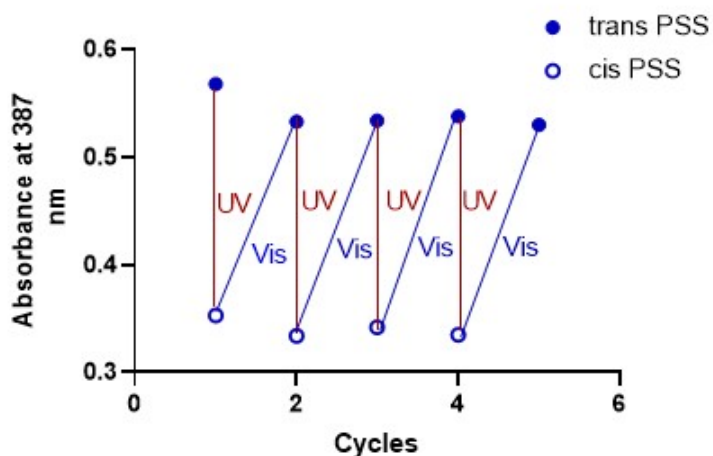


**Figure S3: Photocyclability of *n*-BDAN**

### SANS fitting parameter

The SANS patterns collected for *n*-BDAN were analysed using the built-in models from SASView 4.4.0 (<https://www.sasview.org>). Both models were fit using a scattering length density (SLD) of 1.37 for the micelle core and 6.3 for the D<sub>2</sub>O solvent. The detailed fitting parameters are provided in Table S3.

**Table S3: SANS Fitting parameters**

| Sample               | Model                              | Cylinder length/<br>Polar<br>radius (Å) | Cylinder radius/<br>Equatorial<br>radius (Å) | Axis ratio | Background<br>(1/cm) | Scale  |
|----------------------|------------------------------------|---|--|------------|----------------------|--------|
| <i>trans n</i> -BDAN | Flexible<br>elliptical<br>cylinder | ~2600                                   | 18   | 1.8        | 0.0007               | 0.0024 |
| <i>cis n</i> -BDAN   | Elliptical<br>Cylinder             | 678                                     | 18   | 1.8        | 0.0035               | 0.008  |

\*Kuhn length for *trans n*-BDAN is >1000 Å

### Rheology

Triplicate rheological measurements were performed on a representative 1 wt.% *n*-BDAP sample to evaluate experimental reproducibility. The mean values and corresponding standard

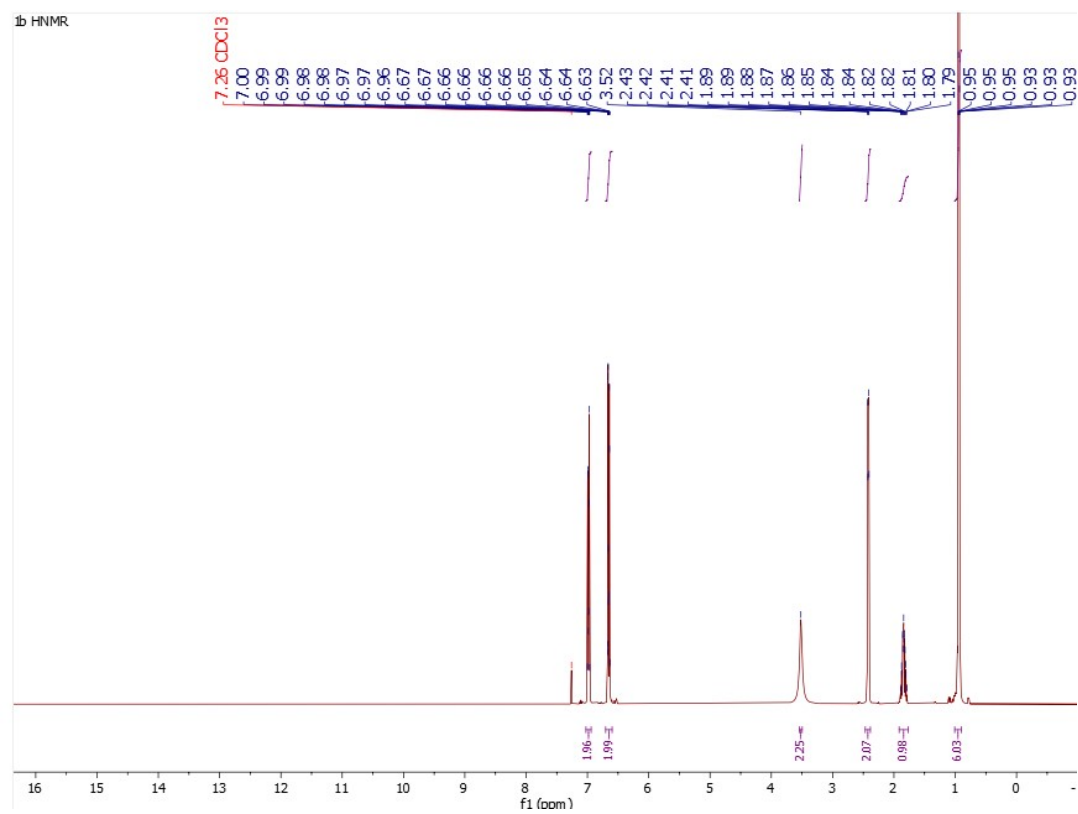
deviations for viscosity, storage modulus, loss modulus, and relaxation time are summarised in Table S4.

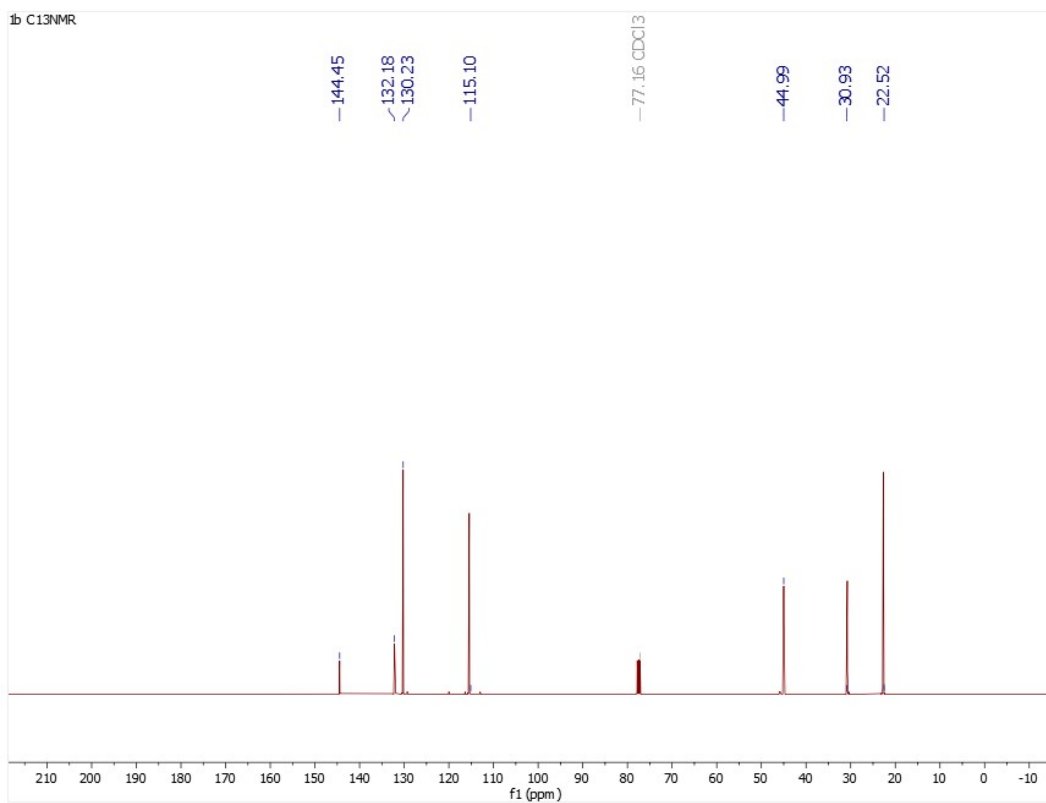
**Table S4.** Mean  $\pm$  SD from triplicate rheological measurements of 1 wt.% n-BDAP.

| Parameter                  | Mean                 | SD                       | Unit  |
|----------------------------|----------------------|--------------------------|-------|
| Viscosity                  | $1.20 \times 10^3$   | $\pm 30.9$               | mPa·s |
| Storage modulus ( $G'$ )   | $1.4 \times 10^{-3}$ | $\pm 7.3 \times 10^{-4}$ | Pa    |
| Loss modulus ( $G''$ )     | $1.3 \times 10^{-3}$ | $\pm 8.3 \times 10^{-4}$ | Pa    |
| Relaxation time ( $\tau$ ) | 0.66                 | $\pm 0.49$               | S     |

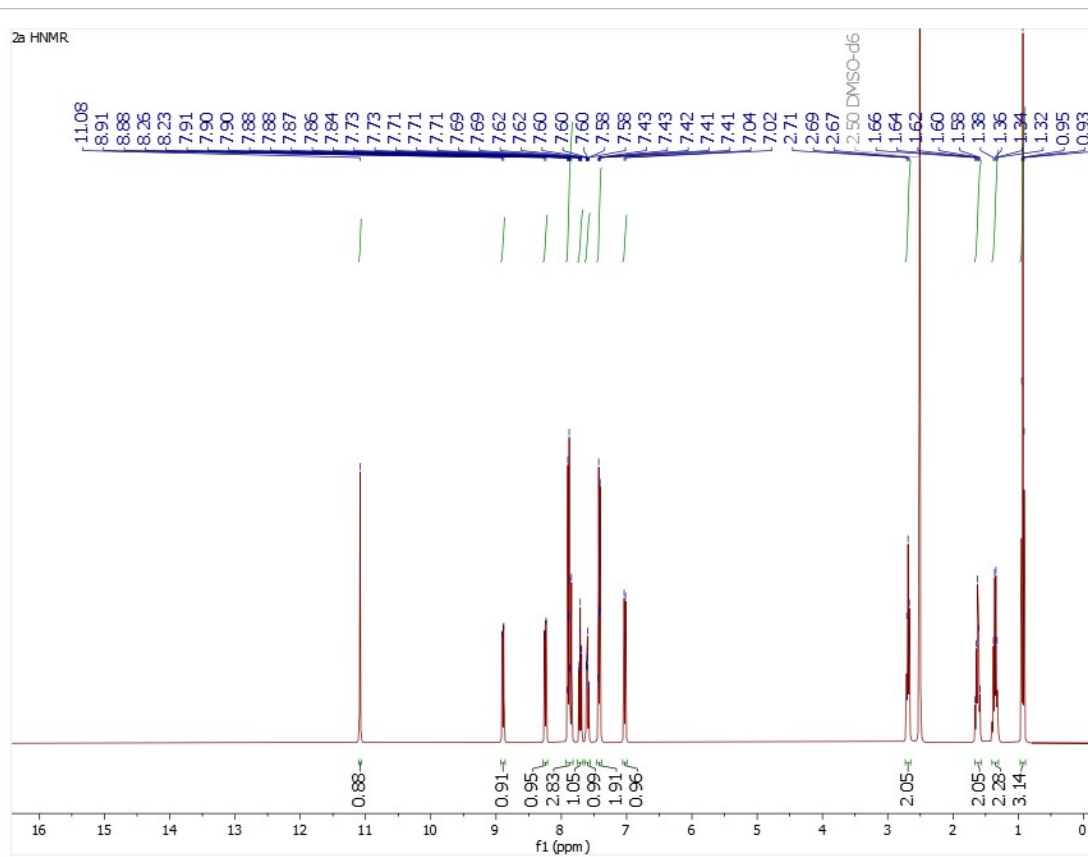
NMR Spectra

1b

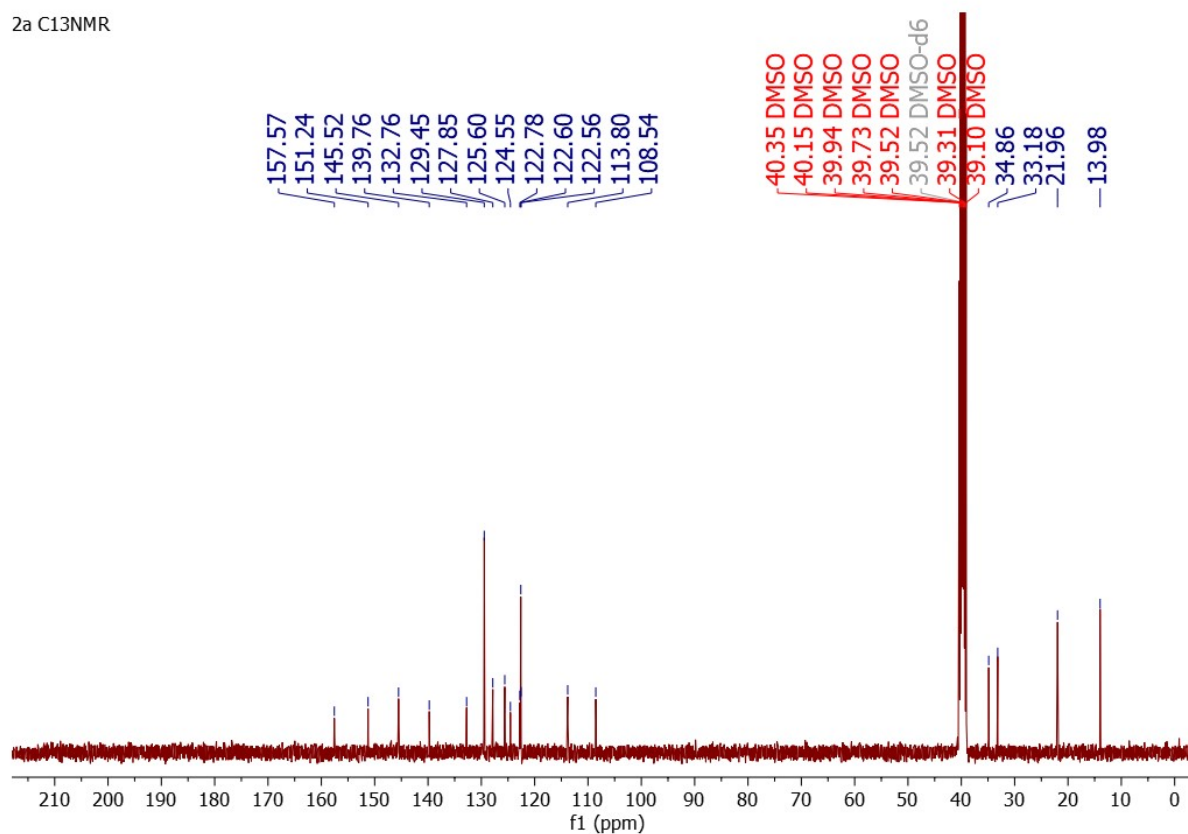




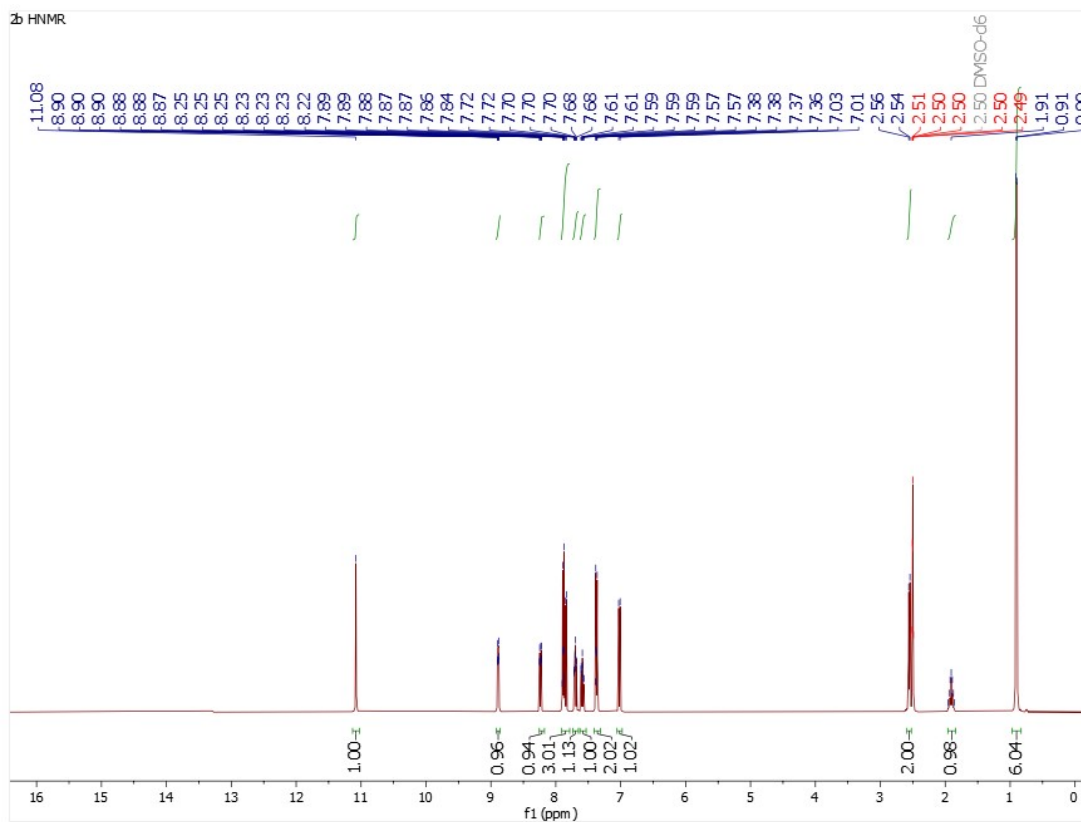
2a

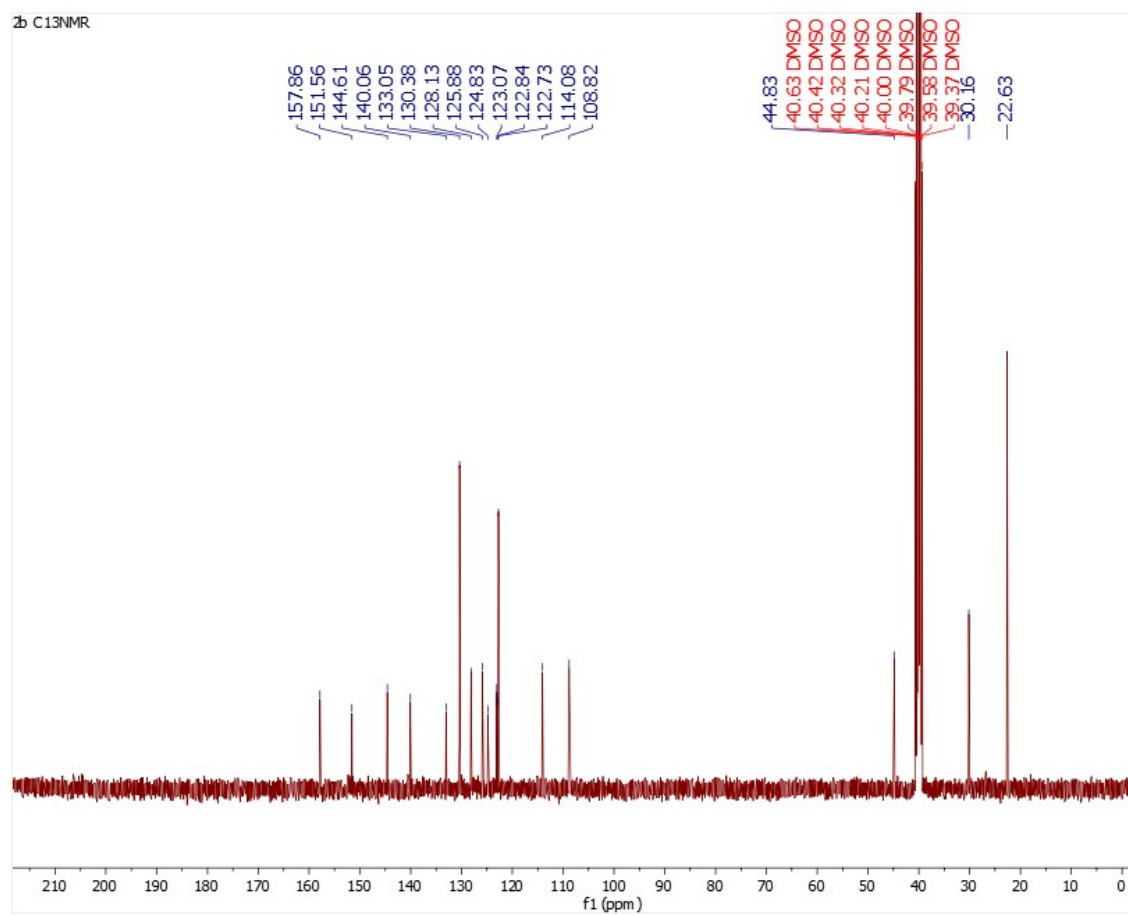


2a C13NMR



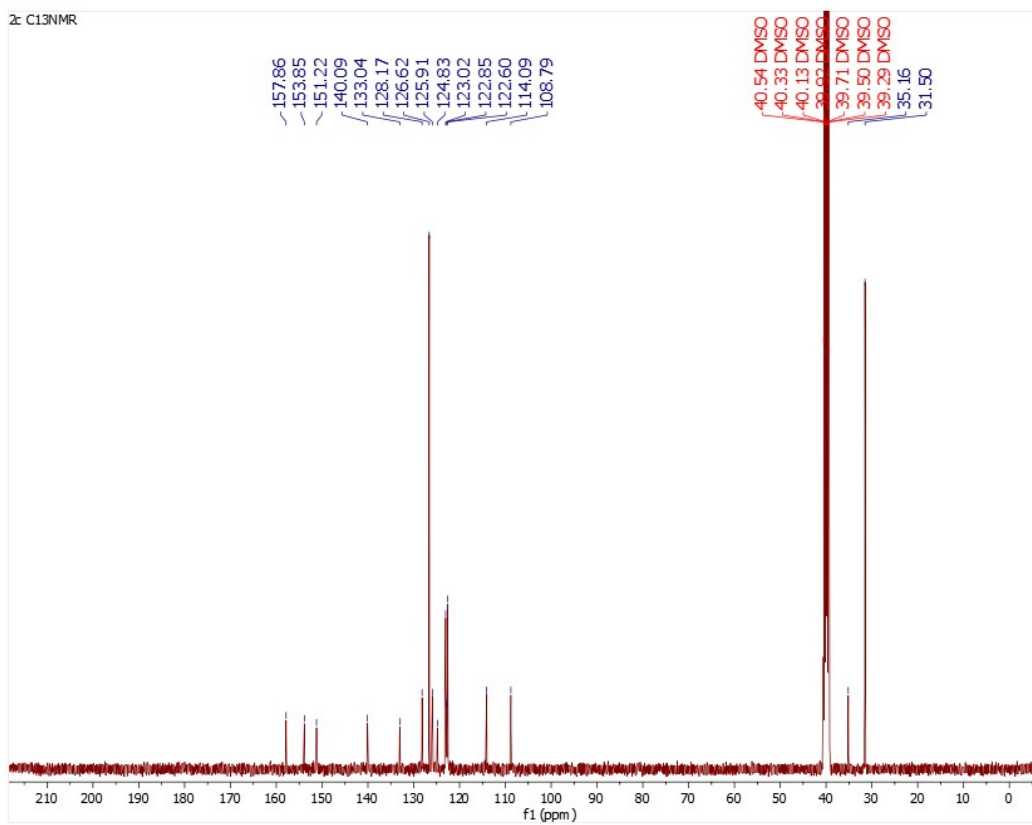
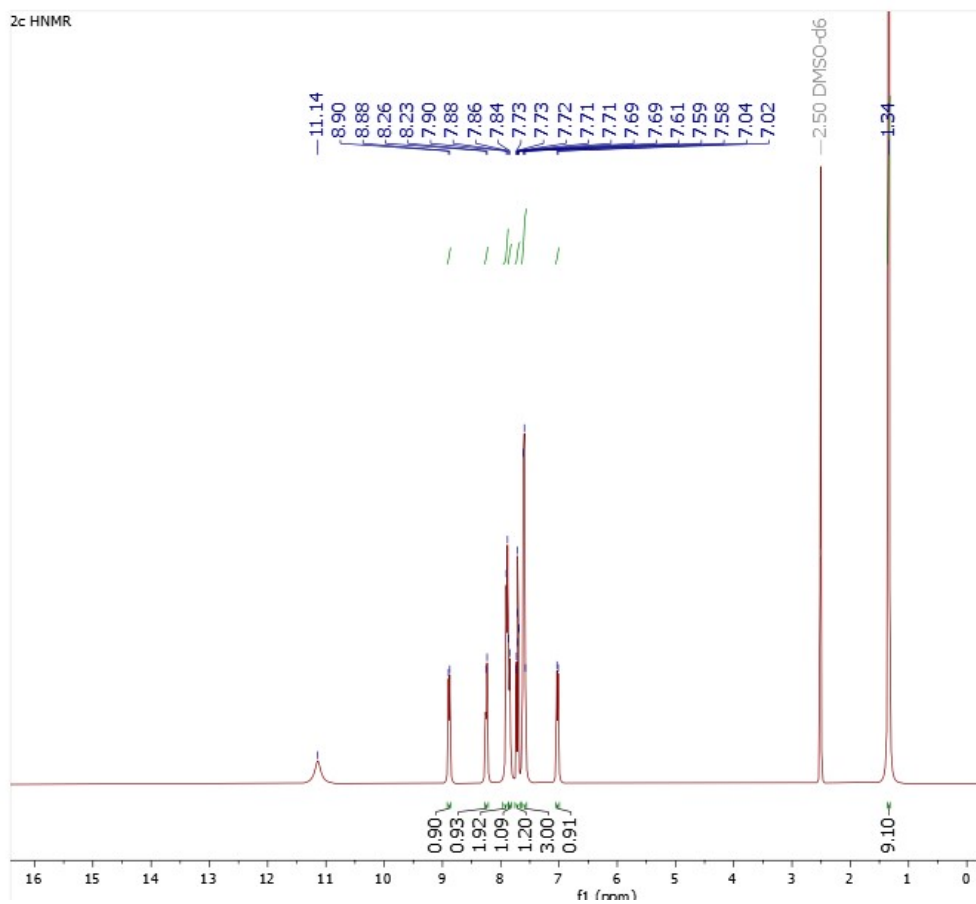
2b



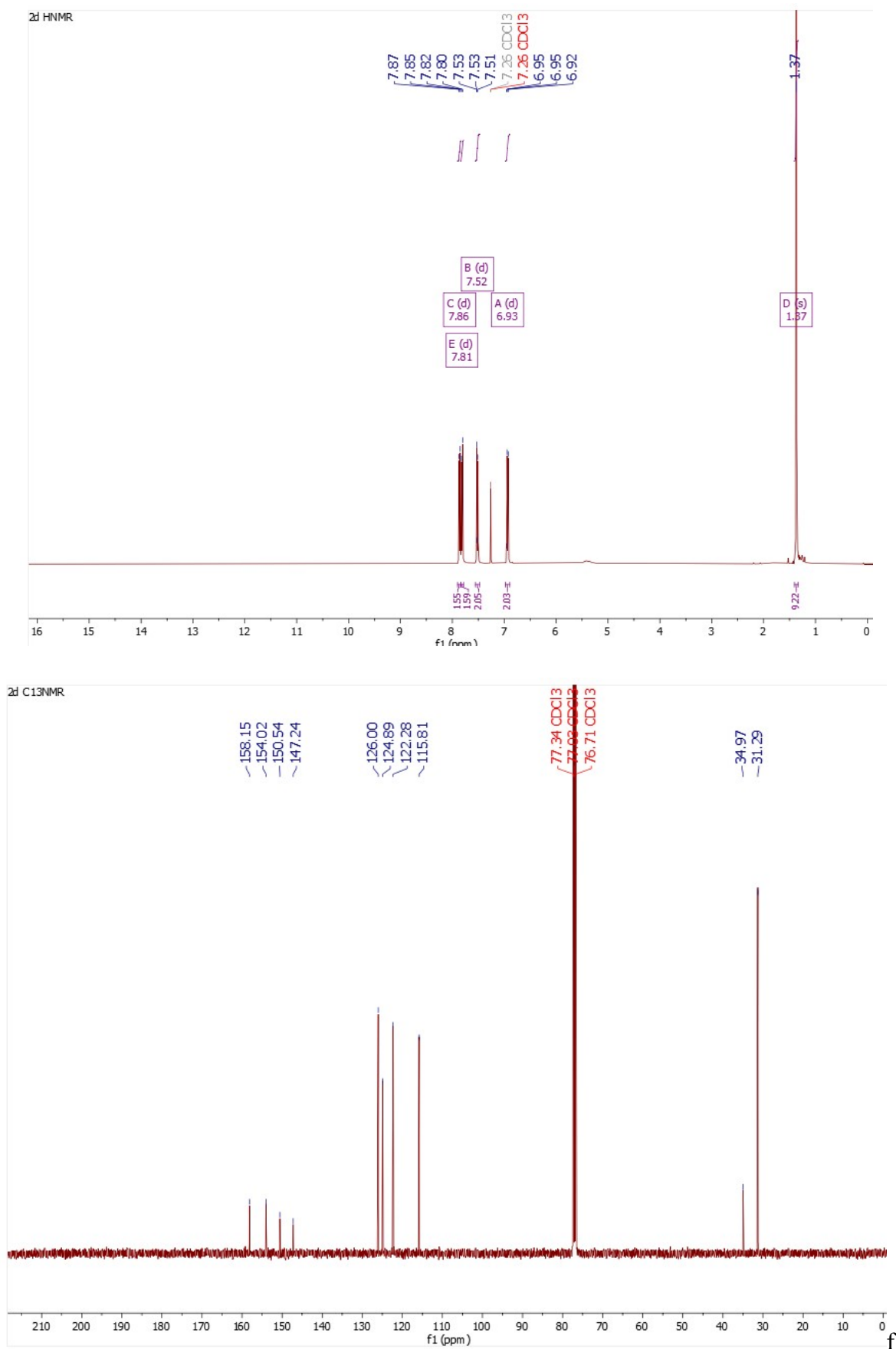


2c



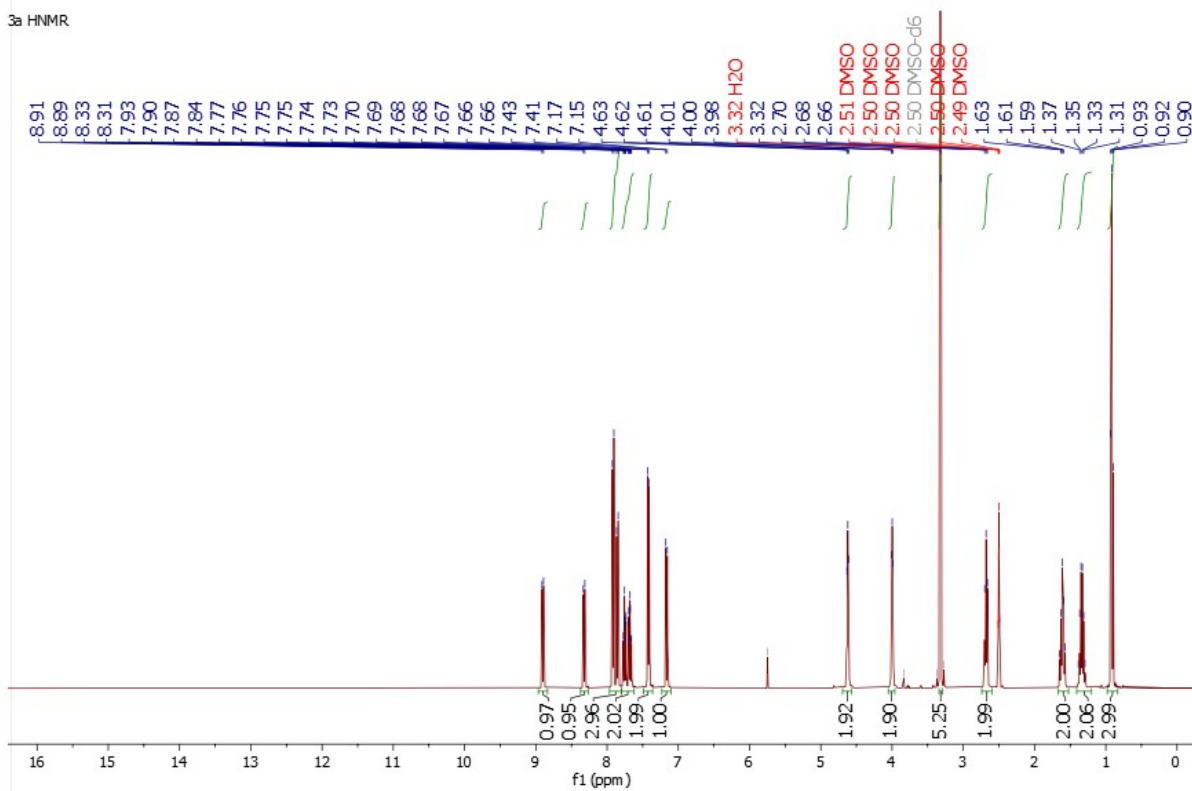


2d

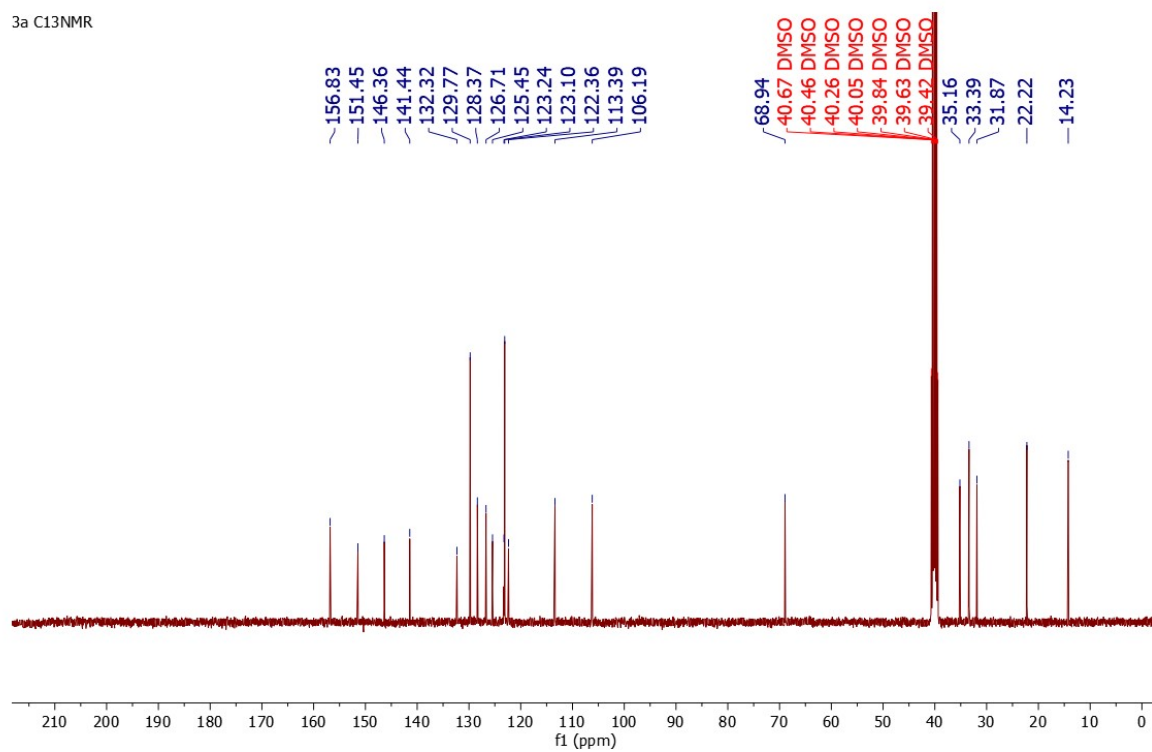


3a

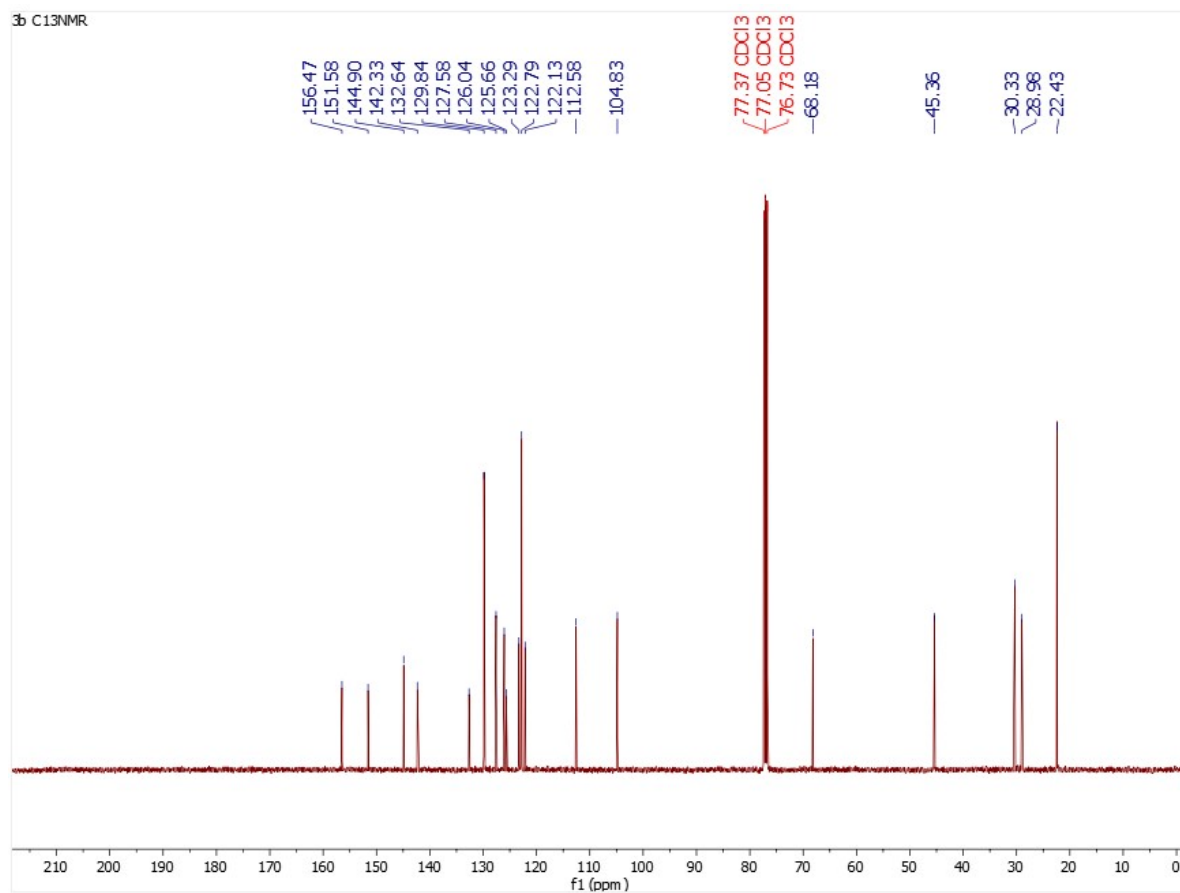
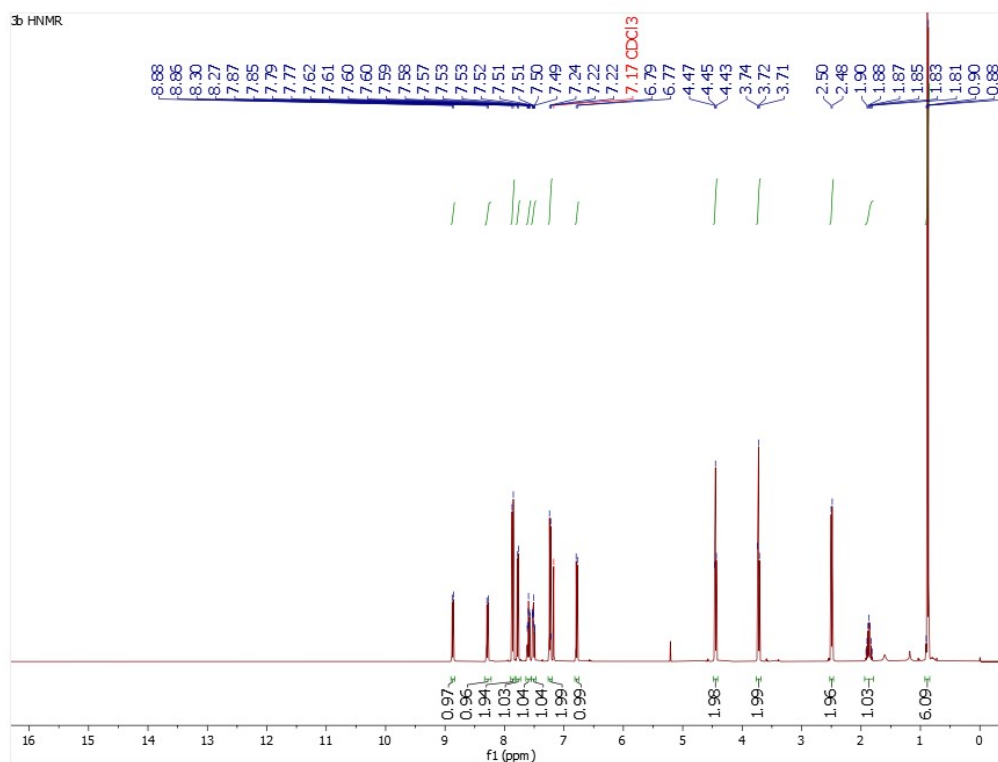
3a <sup>1</sup>H NMR



3a <sup>13</sup>C NMR

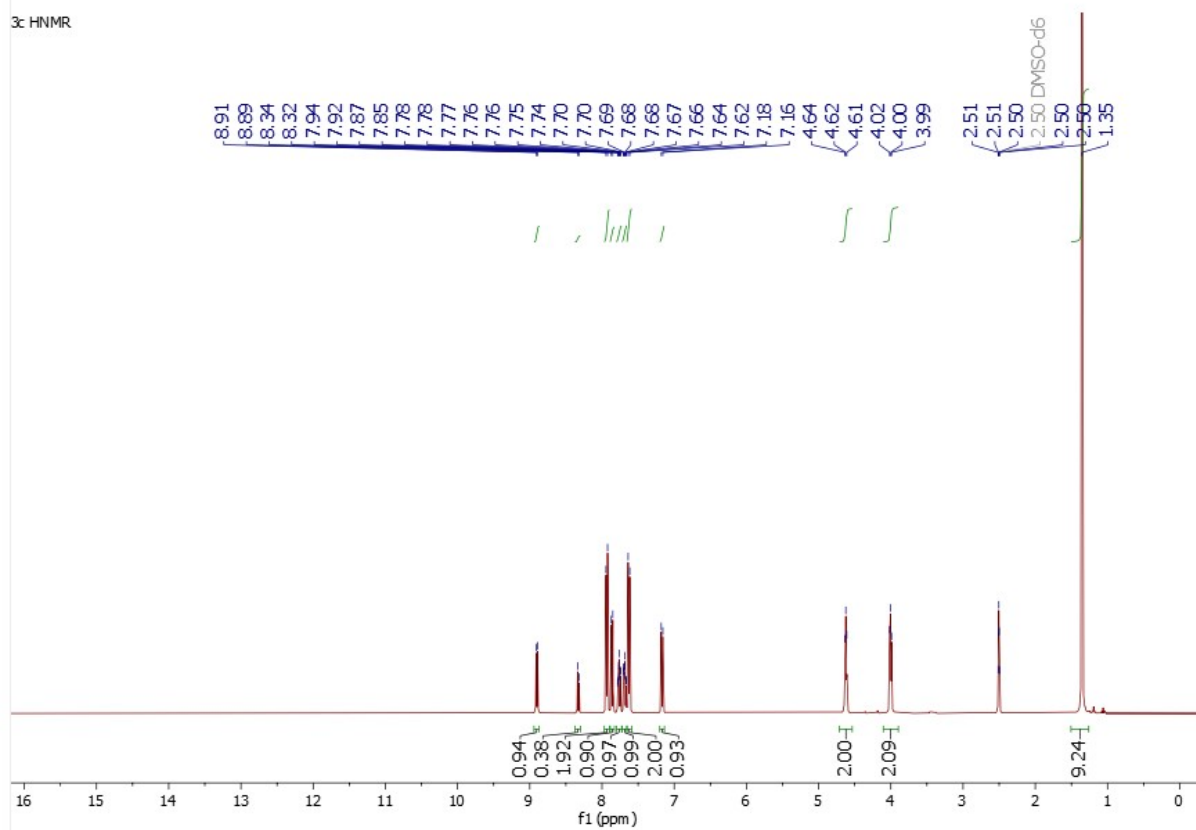


3b

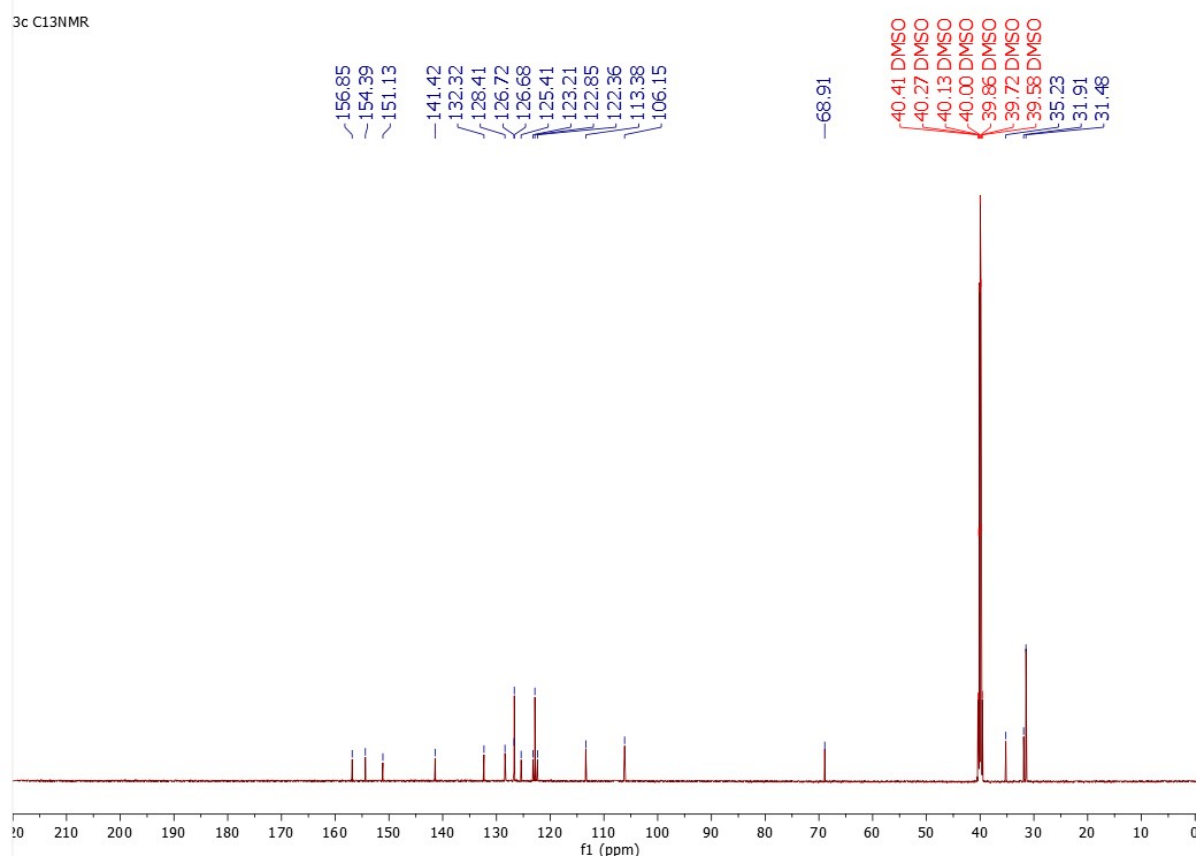


3c

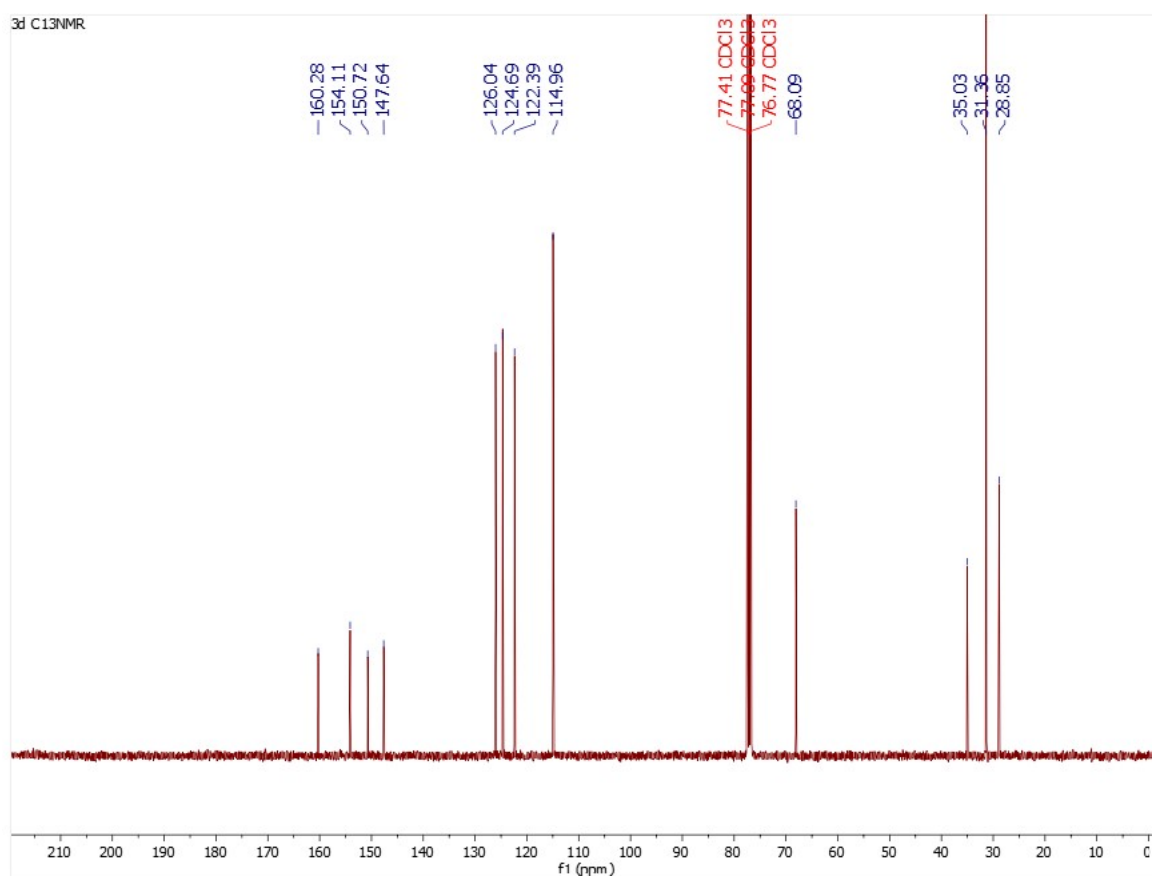
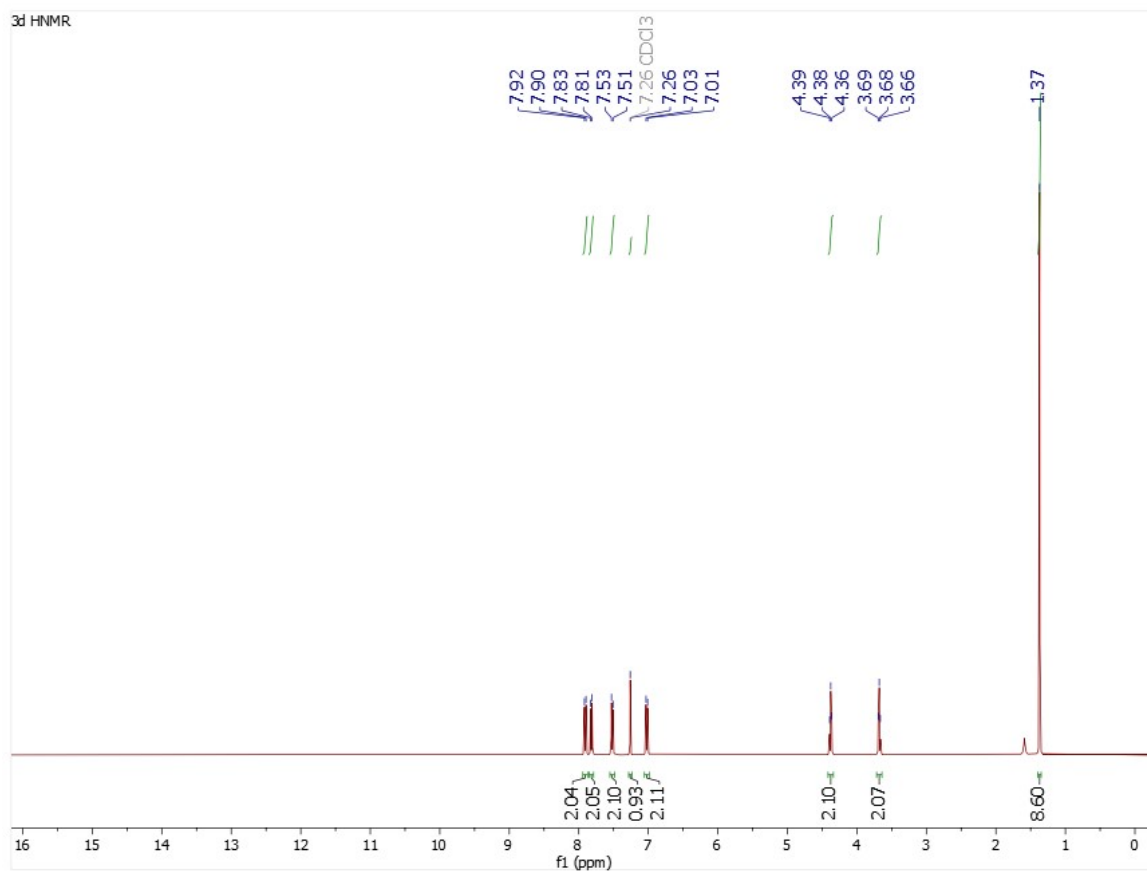
3c <sup>1</sup>H NMR



3c <sup>13</sup>C NMR

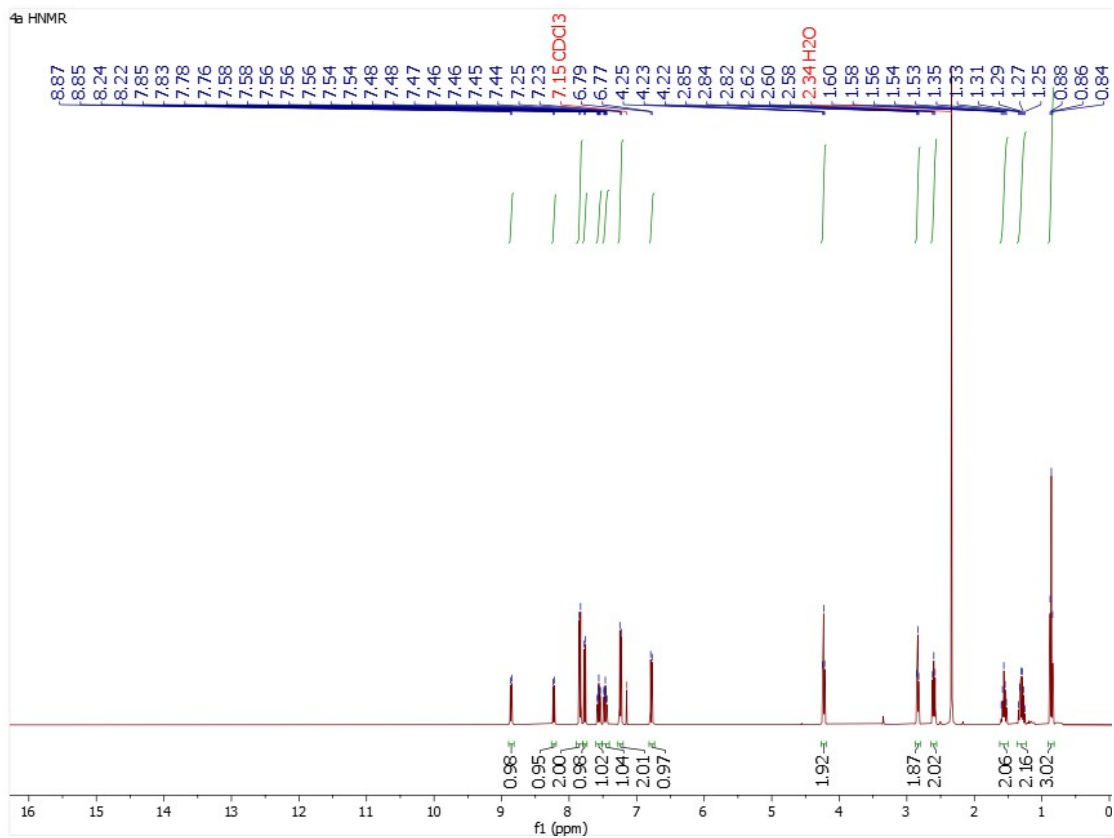


3d

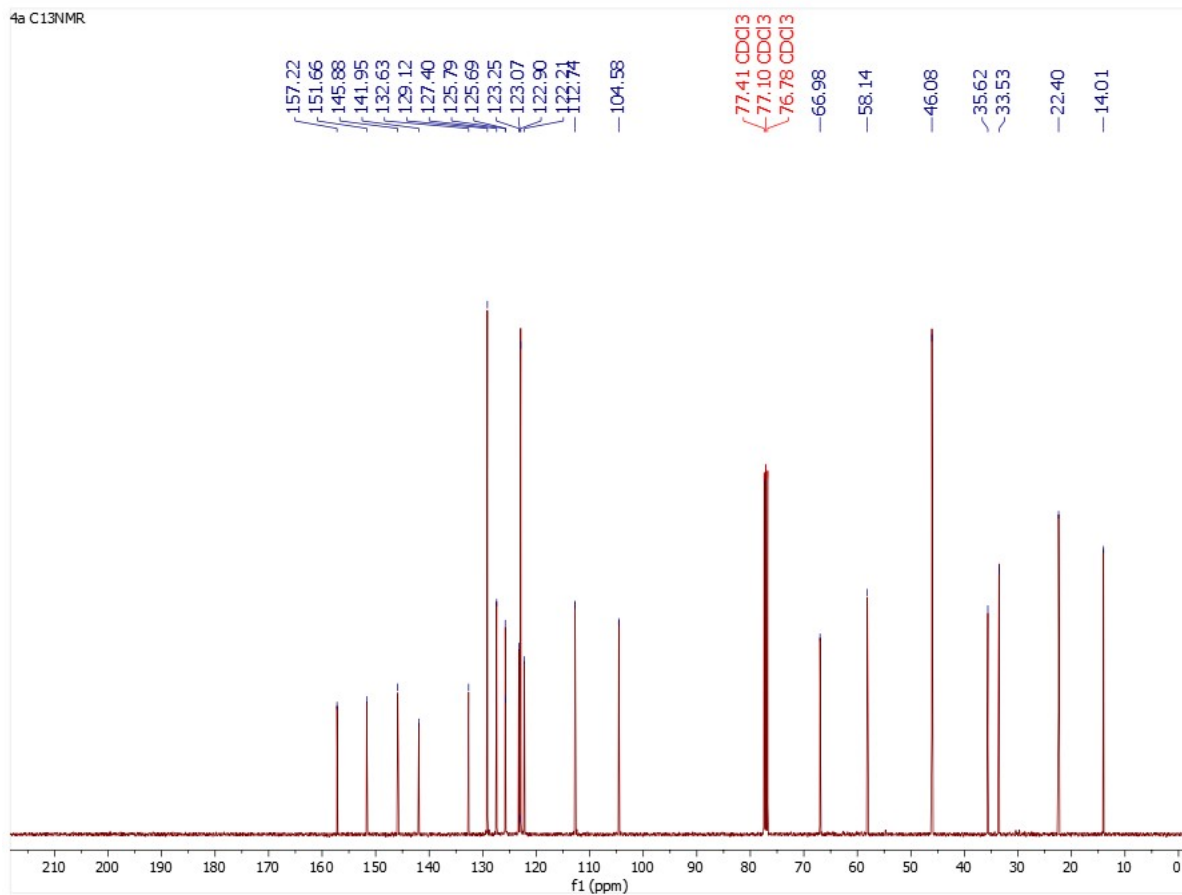


4a

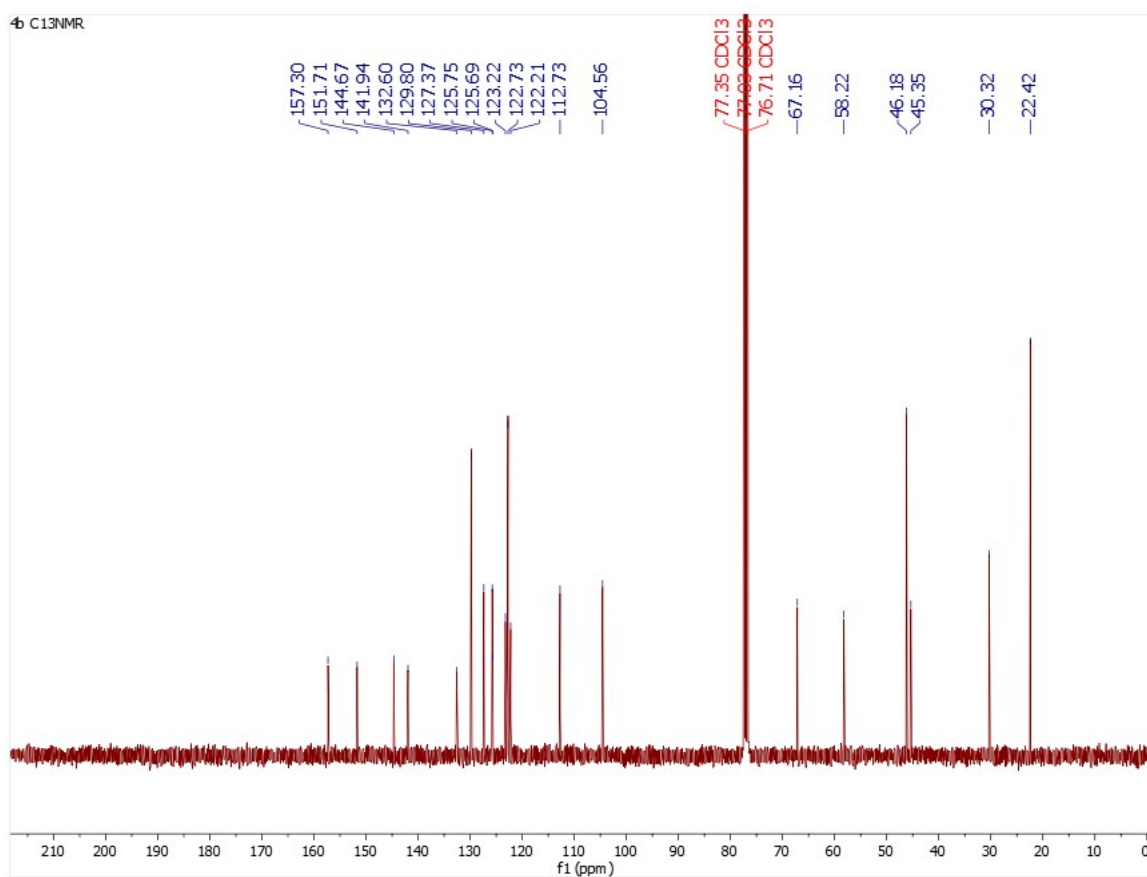
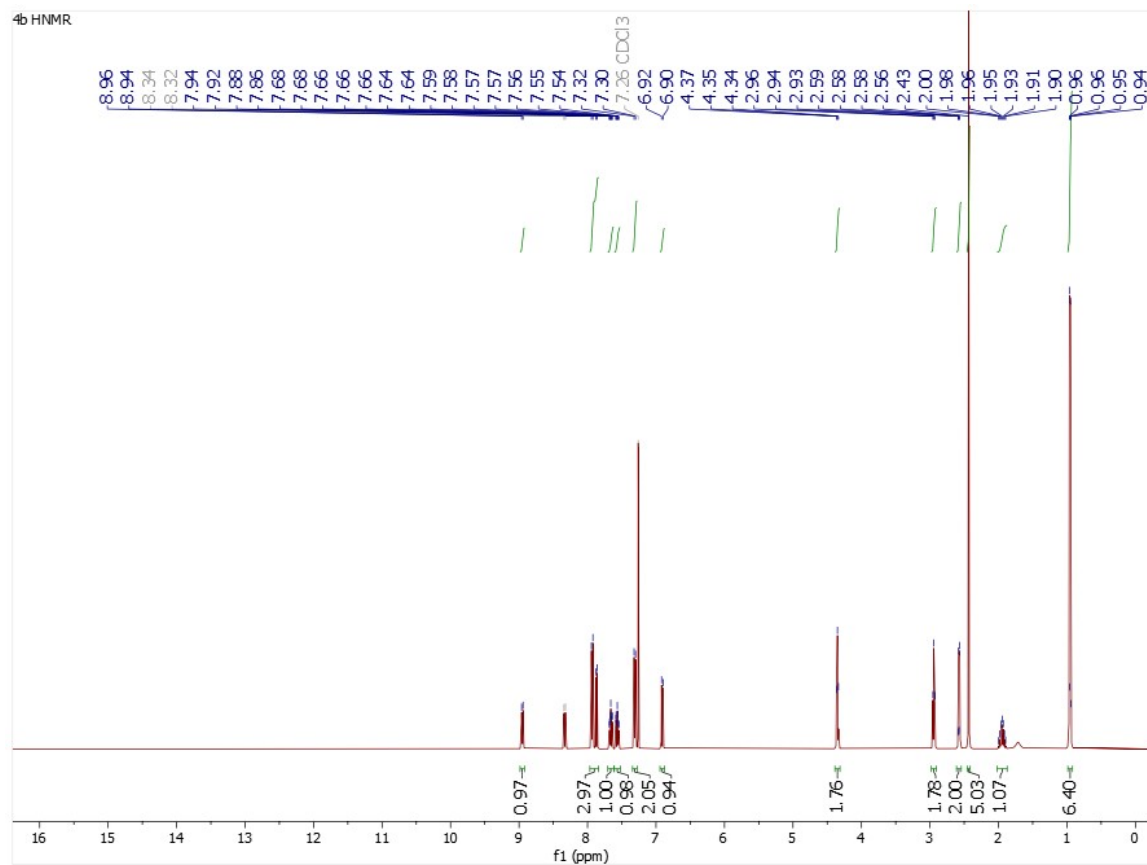
4a HNMR



4a C13NMR

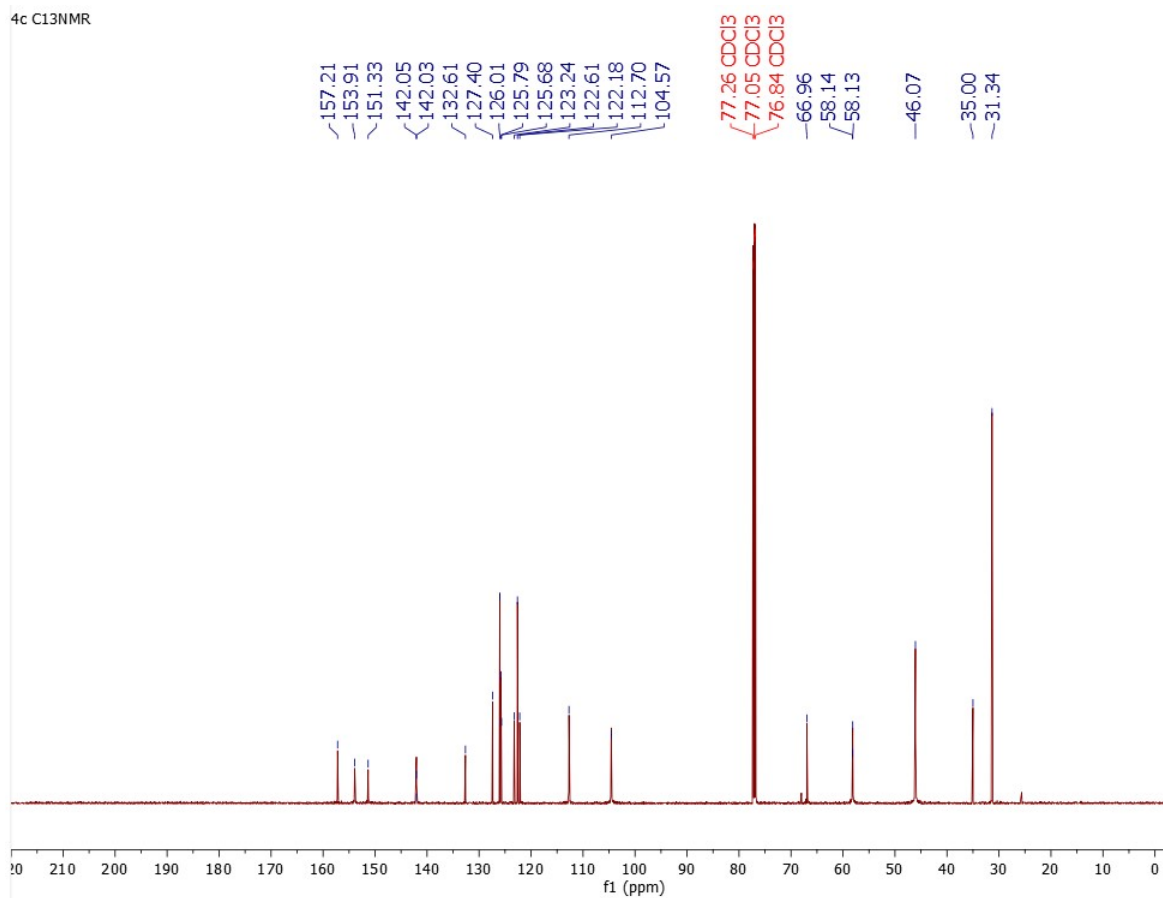
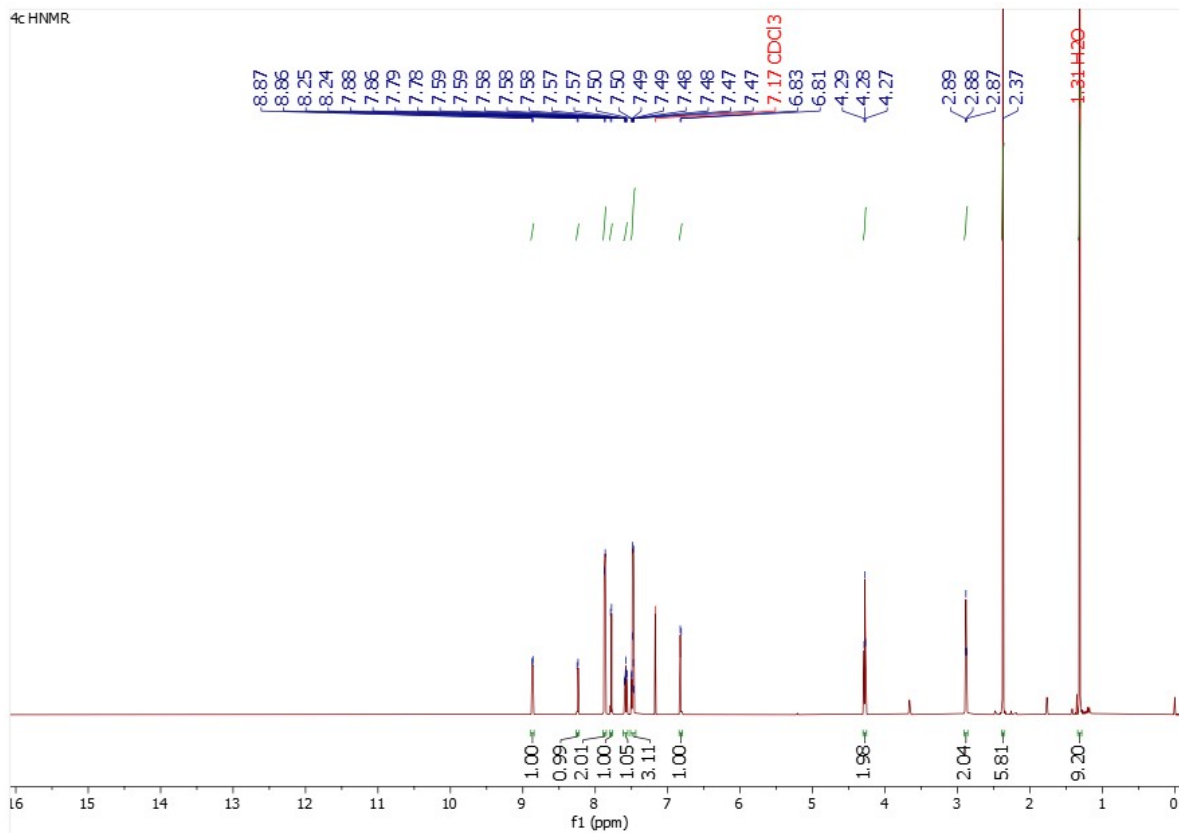


4b

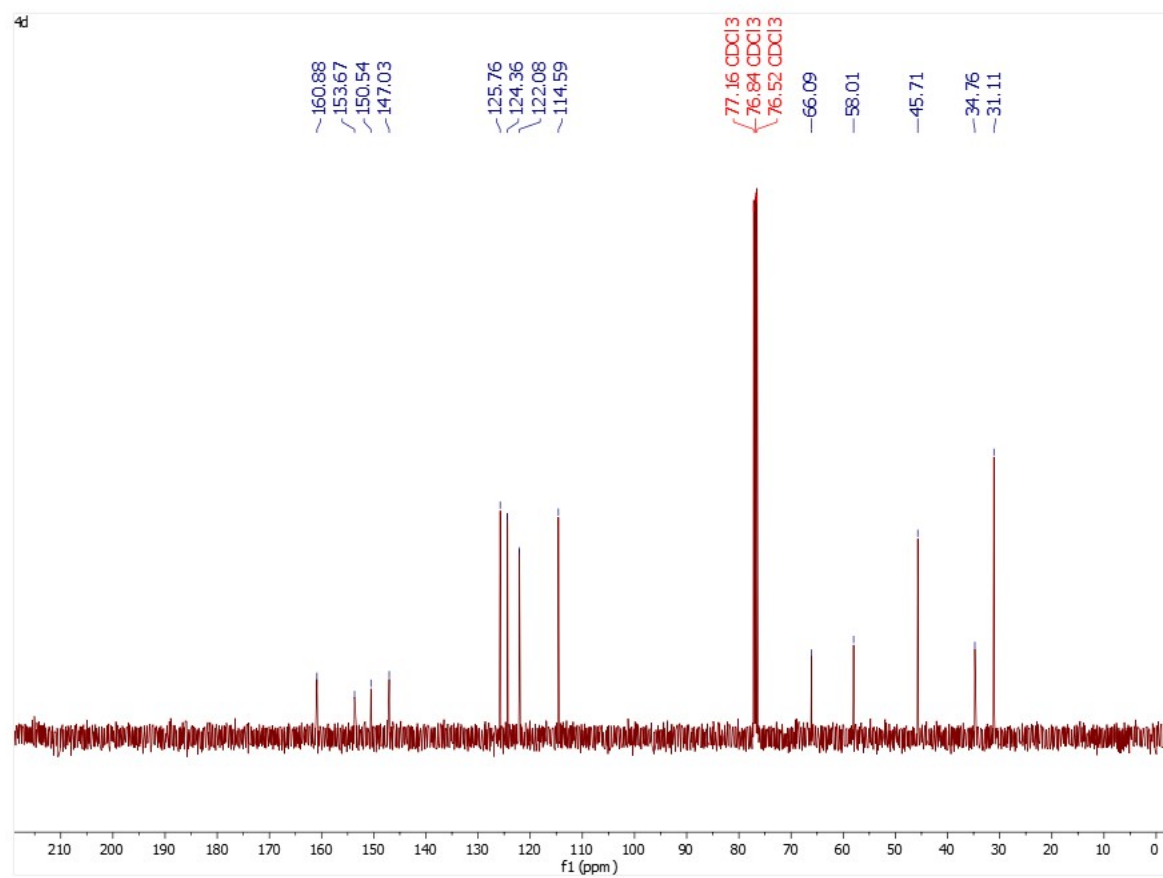
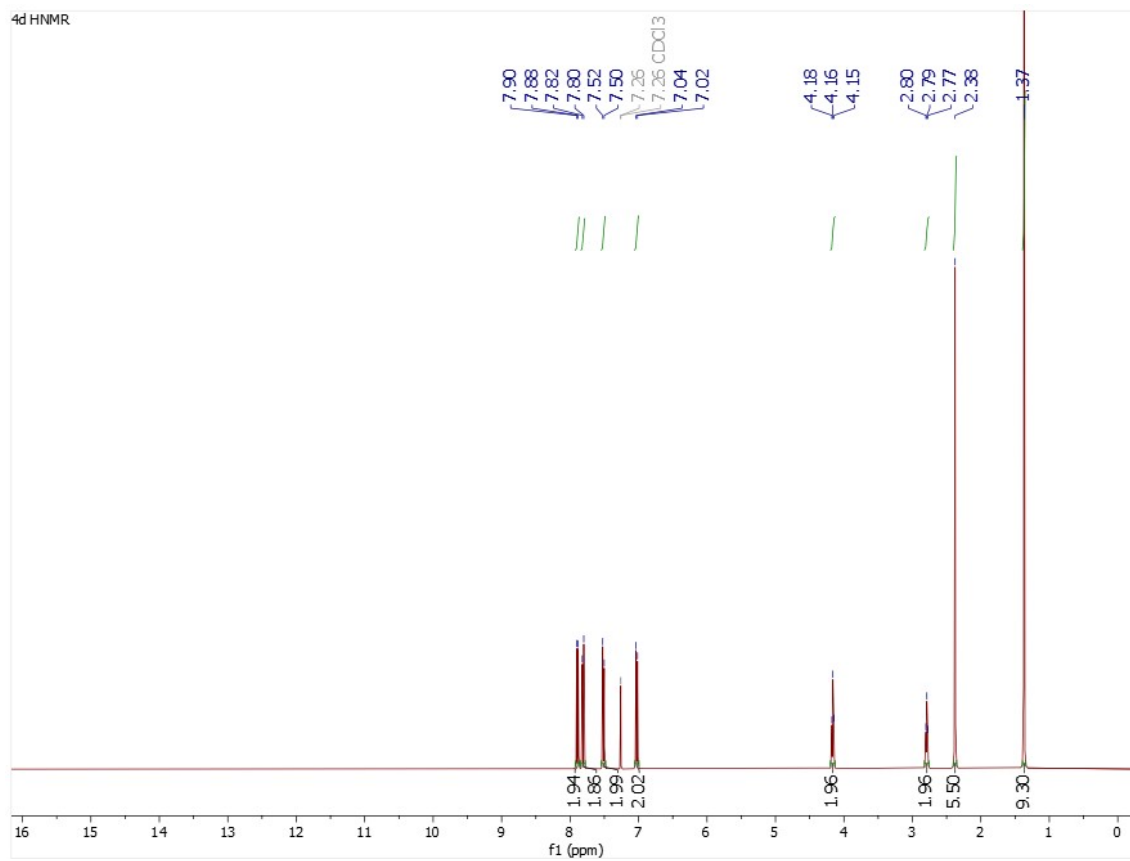


4c

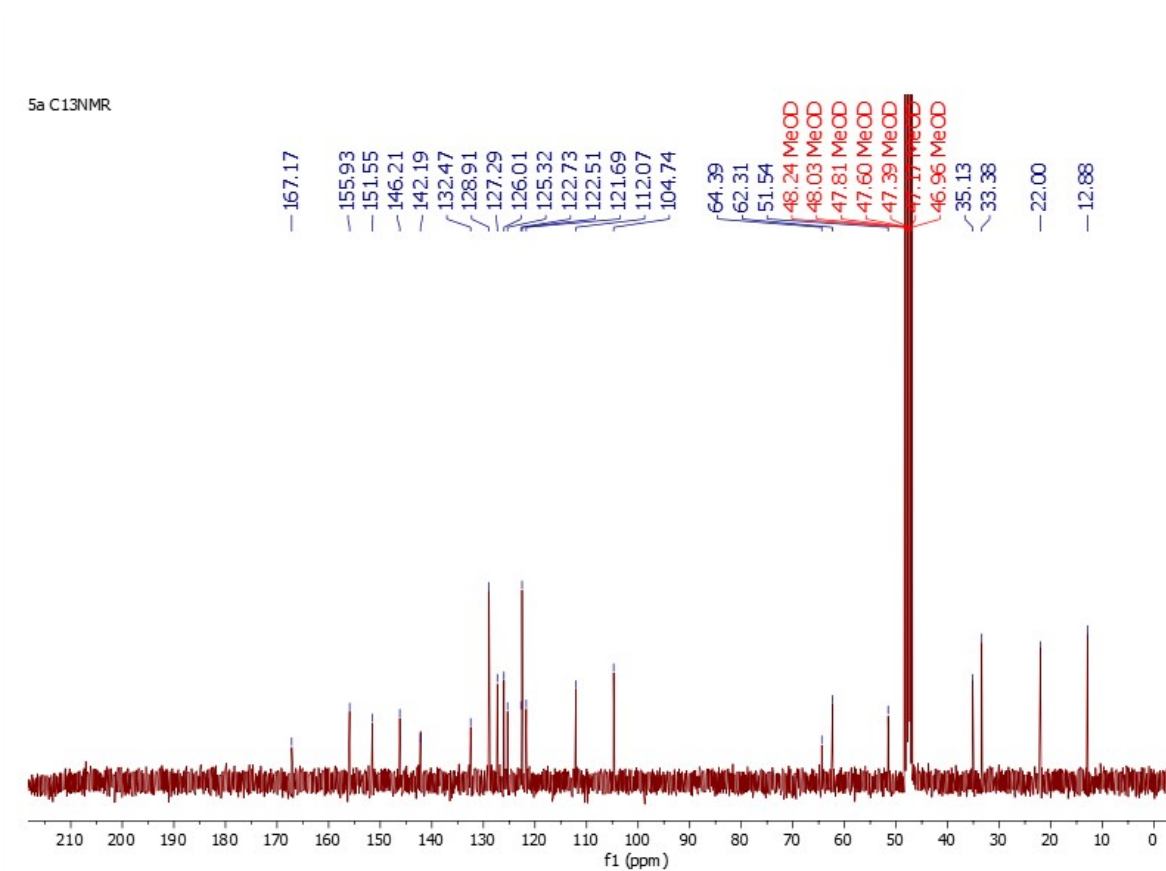
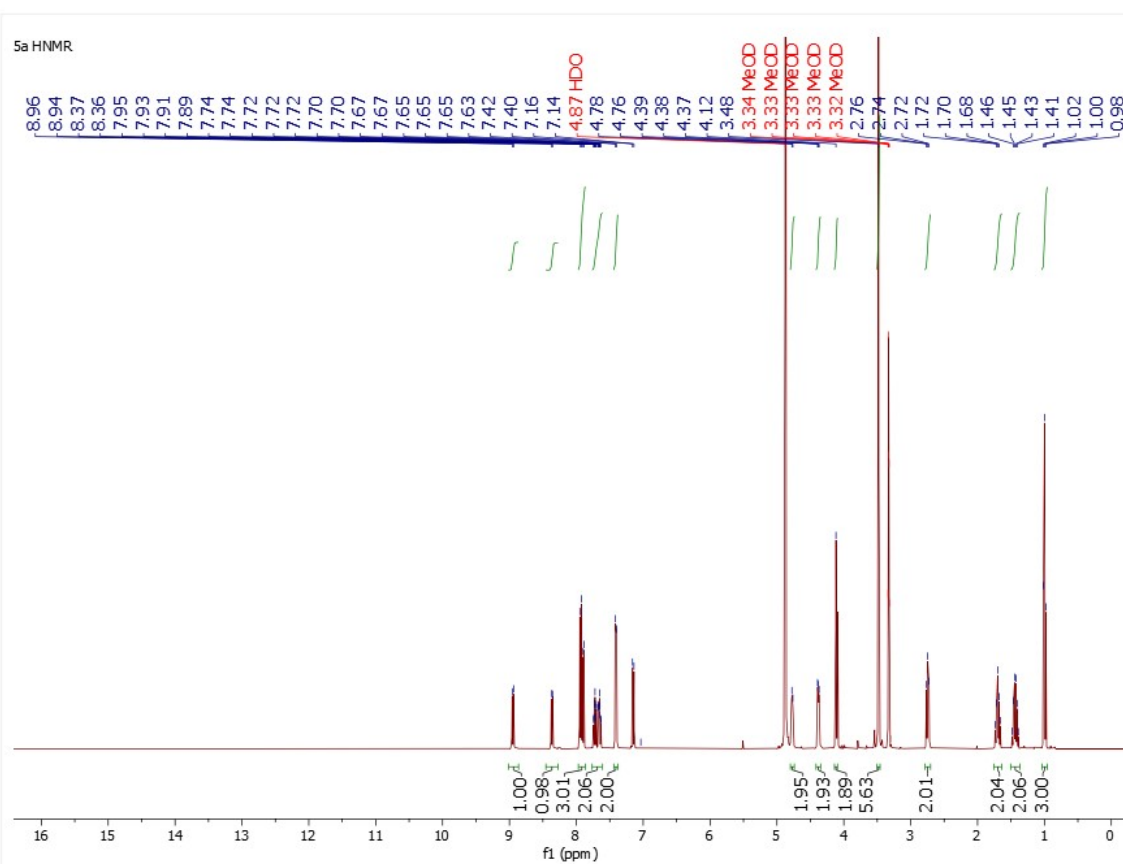




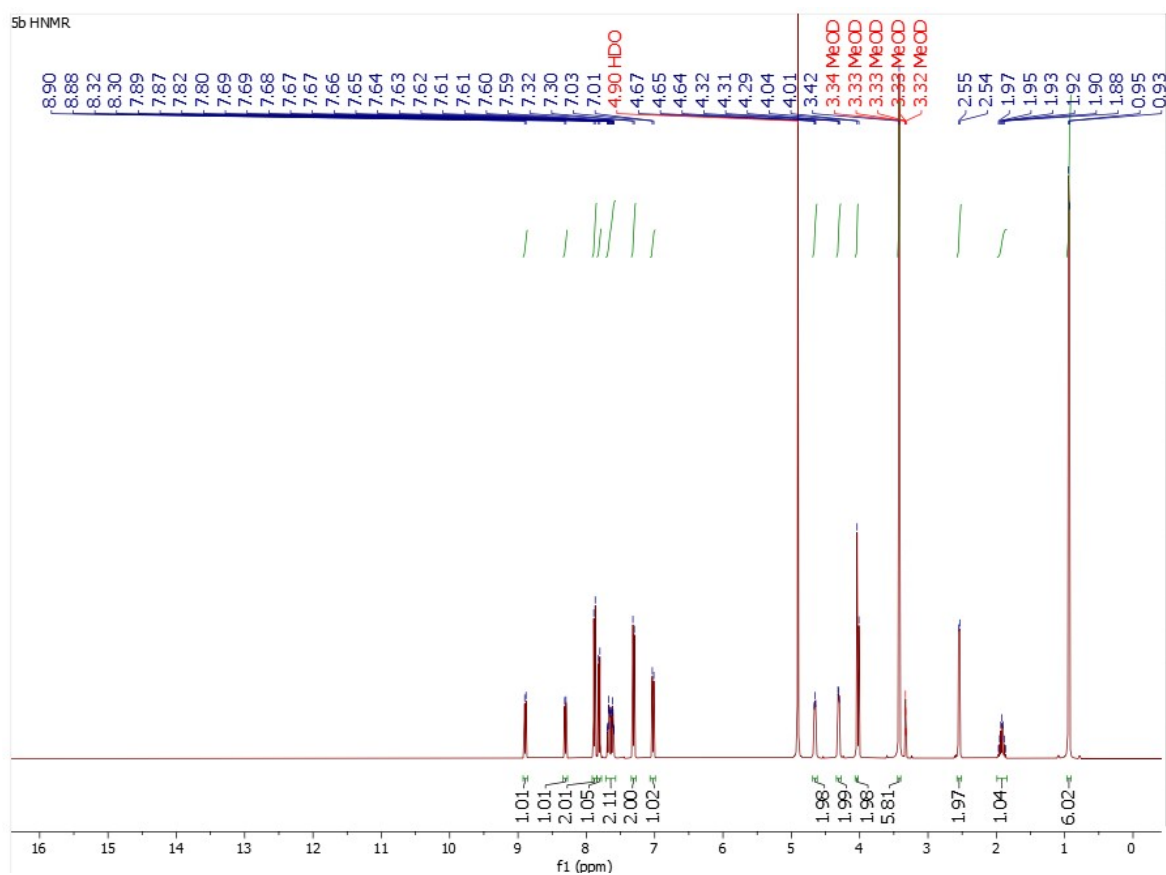
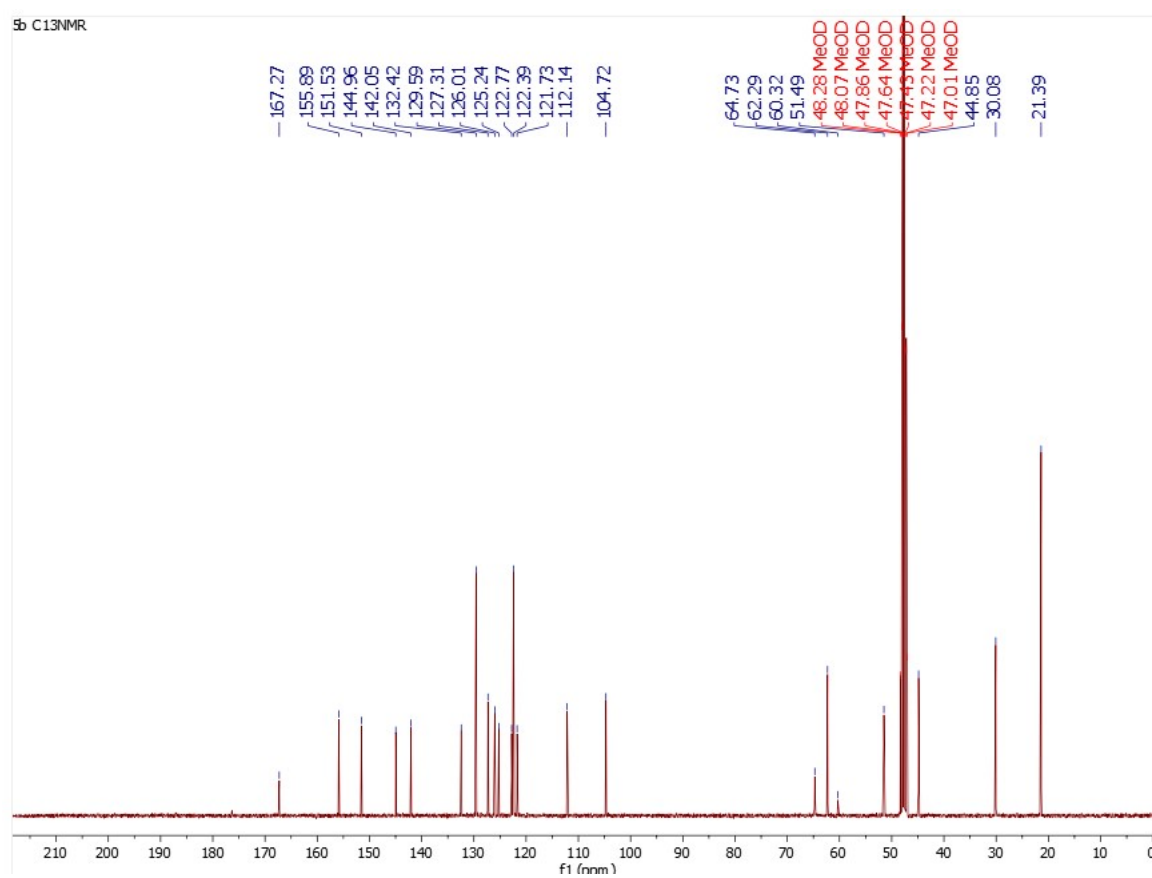
4d

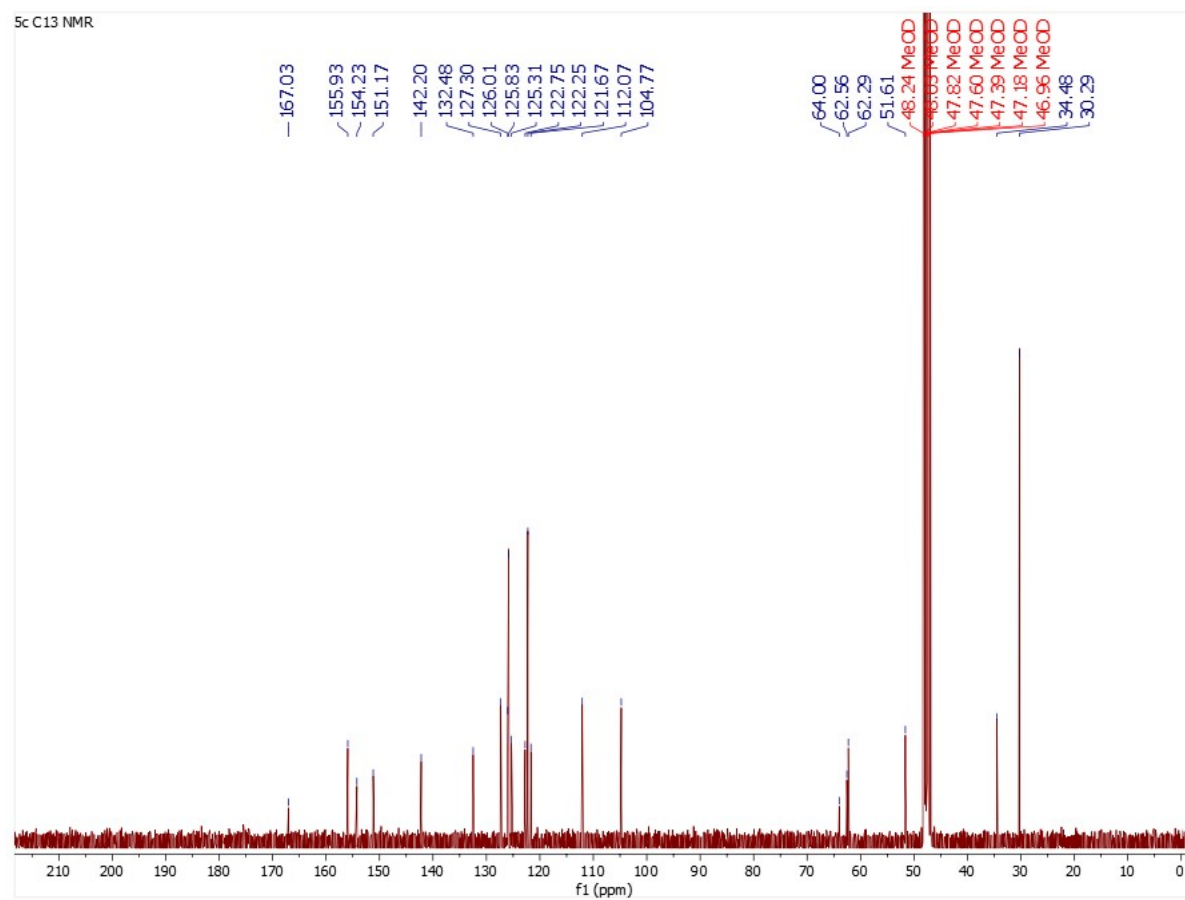
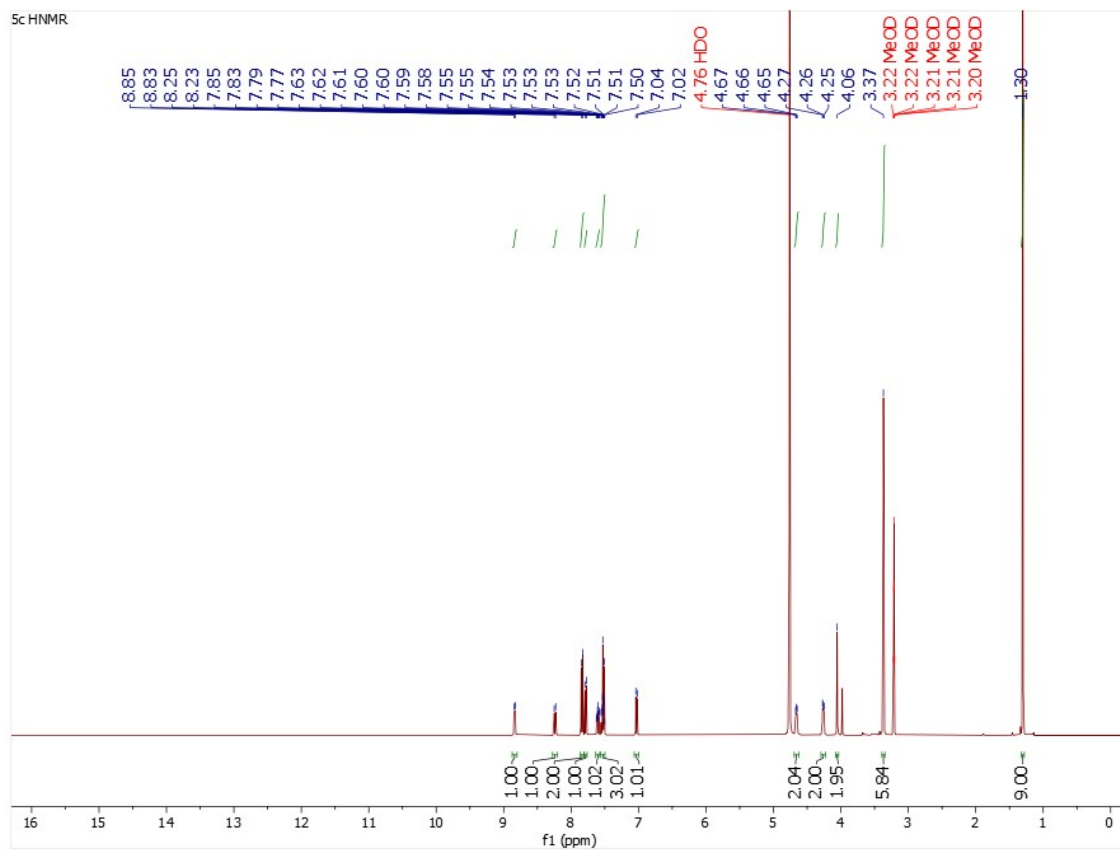


5a

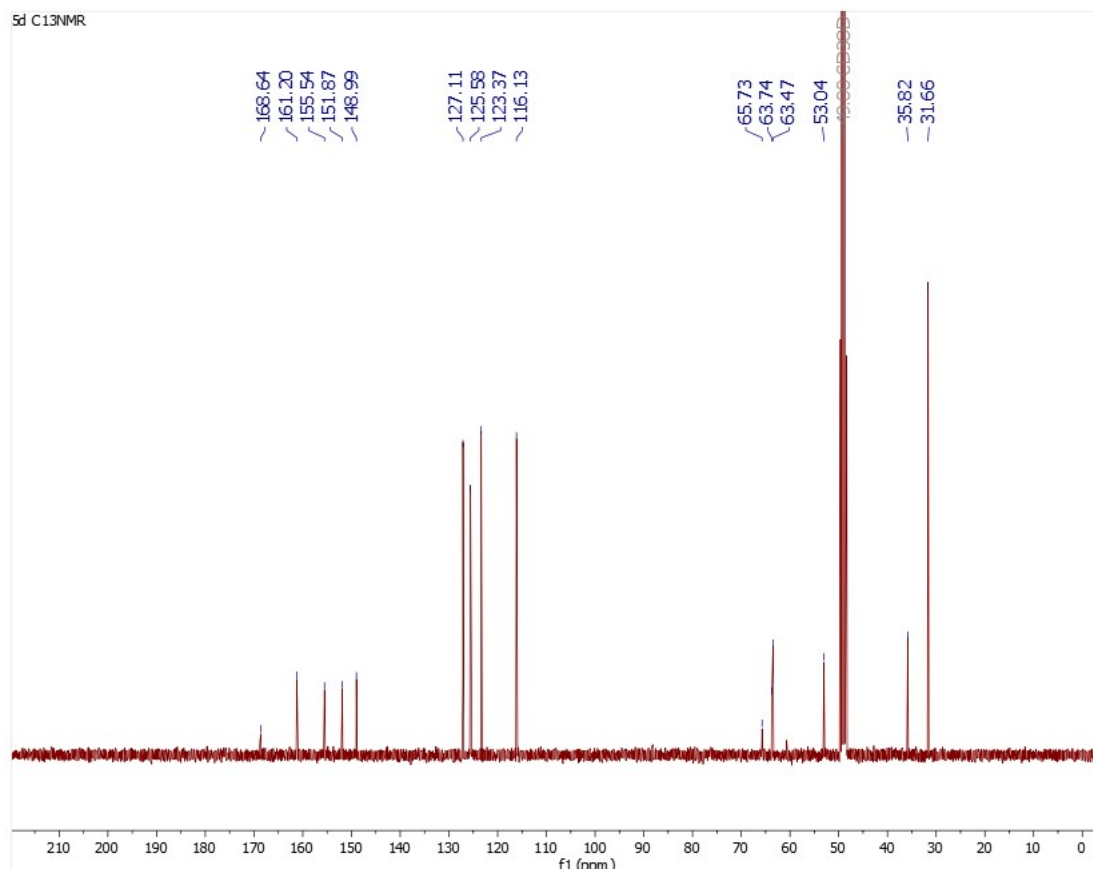
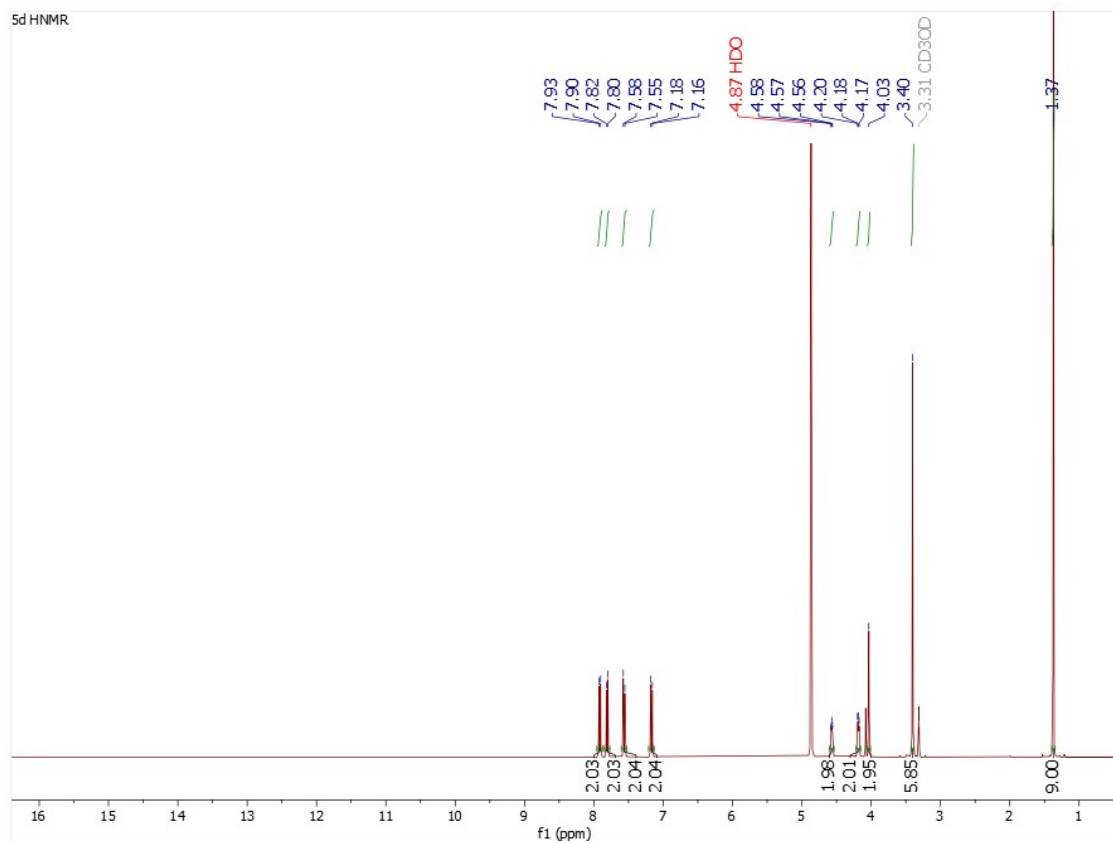


5b

5b <sup>1</sup>H NMR5b <sup>13</sup>C NMR



5d



References

1. Butler, C. S.; Giles, L. W.; Sokolova, A. V.; de Campo, L.; Tabor, R. F.; Tuck, K. L., Structure–Performance Relationships for Tail Substituted Zwitterionic Betaine–Azobenzene Surfactants. *Langmuir* **2022**.
2. Zimmerman, G.; Chow, L.-Y.; Paik, U.-J., The photochemical isomerization of azobenzene. *Journal of the American Chemical Society* **1958**, *80* (14), 3528-3531.
3. Beharry, A. A.; Woolley, G. A., Azobenzene photoswitches for biomolecules. *Chemical Society Reviews* **2011**, *40* (8), 4422-4437.